



Agrohydrological analysis of groundwater recharge and land use changes in
the Pampas of Argentina

Kroes, J., van Dam, J., Supit, I., de Abelleira, D., Verón, S., de Wit, A., ...
Veldhuizen, A.

This is a "Post-Print" accepted manuscript, which has been published in "Agricultural
Water Management"

This version is distributed under a non-commercial no derivatives Creative Commons



(CC-BY-NC-ND) user license, which permits use, distribution, and
reproduction in any medium, provided the original work is properly cited and not
used for commercial purposes. Further, the restriction applies that if you remix,
transform, or build upon the material, you may not distribute the modified material.

Please cite this publication as follows:

Kroes, J., van Dam, J., Supit, I., de Abelleira, D., Verón, S., de Wit, A., ...
Veldhuizen, A. (2019). Agrohydrological analysis of groundwater recharge and land
use changes in the Pampas of Argentina. *Agricultural Water Management*, 213, 843-
857. DOI: 10.1016/j.agwat.2018.12.008

You can download the published version at:

<https://doi.org/10.1016/j.agwat.2018.12.008>

1 Agrohdrological analysis of groundwater recharge and land use changes in the Pampas of
2 Argentina

3
4 *Joop Kroes, Jos van Dam, Iwan Supit, Diego de Abelleyra, Santiago Verón, Allard de Wit, Hendrik*
5 *Boogaard, Marcos Angelini, Francisco Damiano, Piet Groenendijk, Jan Wesseling, Ab Veldhuizen*

6
7
8 J.G. (Joop) Kroes: Wageningen University and Research, chair Soil Physics and Land Management, P.O. Box
9 47, 6700 AA Wageningen, The Netherlands. joop.kroes@wur.nl

10
11 J.C. (Jos) van Dam: Wageningen University and Research, chair Soil Physics and Land Management, P.O. Box
12 47, 6700 AA Wageningen, The Netherlands. jos.vandam@wur.nl

13
14 I. (Iwan) Supit: Wageningen University and Research, chair Water Systems and Global Change, P.O. Box 47,
15 6700 AA Wageningen, The Netherlands. iwan.supit@wur.nl

16
17 D. (Diego) De Abelleyra: Instituto Nacional de Tecnología Agropecuaria (INTA). Instituto de Clima y Agua –
18 Castelar. N. Repetto y De Los Reseros s/n° (B1686WAA), Hurlingham, Buenos Aires, Argentina.
19 deabelle@gmail.com

20
21 S.R. (Santiago) Verón: Instituto Nacional de Tecnología Agropecuaria (INTA). Instituto de Clima y Agua –
22 Castelar. N. Repetto y De Los Reseros s/n° (B1686WAA), Hurlingham, Buenos Aires, Argentina. FAUBA –
23 CONICET. veron@agro.uba.ar

24
25 A.J.W. (Allard) de Wit: Wageningen University and Research, Wageningen Environmental Research, Unit Earth
26 Observation and Environmental Informatics, P.O. Box 47, 6700 AA Wageningen, The Netherlands.
27 allard.dewit@wur.nl

28
29 H.L. (Hendrik) Boogaard: Wageningen University and Research, Wageningen Environmental Research, Unit
30 Earth Observation and Environmental Informatics, P.O. Box 47, 6700 AA Wageningen, The Netherlands.
31 hendrik.boogaard@wur.nl

32
33 M.E. (Marcos) Angelini: Instituto Nacional de Tecnología Agropecuaria (INTA). Instituto de Suelos –Castelar.
34 N. Repetto y De Los Reseros s/n° (B1686WAA), Hurlingham, Buenos Aires, Argentina.
35 angelini.marcos@inta.gob.ar

36
37 F. (Francisco) Damiano: Instituto Nacional de Tecnología Agropecuaria (INTA). Instituto de Clima y Agua –
38 Castelar. N. Repetto y De Los Reseros s/n° (B1686WAA), Hurlingham, Buenos Aires, Argentina.
39 Damiano.Francisco@inta.gob.ar

40
41 P. (Piet) Groenendijk: Wageningen University and Research, Wageningen Environmental Research, Unit
42 Sustainable Soil Use, P.O. Box 47, 6700 AA Wageningen, The Netherlands. piet.groenendijk@wur.nl

43
44 J.G. (Jan) Wesseling: Wageningen University and Research, chair Soil Physics and Land Management, P.O. Box
45 47, 6700 AA Wageningen, The Netherlands. jan.wesseling@wur.nl

46
47 A.A. (Ab) Veldhuizen: Wageningen University and Research, Wageningen Environmental Research, Unit Soil,
48 Water and Land Dynamics, P.O. Box 47, 6700 AA Wageningen, The Netherlands. ab.veldhuizen@wur.nl

Abstract:

53 This paper studies the changes of groundwater, climate and land use in the Pampas of Argentina.
54 These changes offer opportunities and threats. Lowering groundwater without irrigation causes
55 drought and successive crop and yield damage. Rising groundwater may alleviate drought as capillary
56 rise supports root water uptake and crop growth, thus narrowing the difference between potential and
57 actual yields. However, rising groundwater may also limit soil water storage, cause flooding in
58 metropolitan areas and have a negative impact on crop yields. Changing land use from continuous soy
59 bean into crop rotations or natural vegetation may decrease groundwater recharge and thus decrease
60 groundwater levels. In case of crop rotation however, leaching of nutrients like nitrate may increase.
61 We quantified these impacts using integrated dynamic crop growth and soil hydrology modelling. The
62 models were tested at field scale using a local dataset from Argentina. We applied distributed
63 modelling at regional scale to evaluate the impacts on groundwater recharge and crop yields using
64 long term weather data.
65 The experiments showed that threats arise from continuous monotone land use. Opportunities are
66 created when a proper balance is found between supply and demand of soil water using a larger
67 differentiation of land use. Increasing the areas of land use types with higher evapotranspiration, like
68 permanent grassland and trees, will contribute to a more stable hydrologic system with more water
69 storage capacities in the soil system and lower groundwater levels.
70 Modelling tools clearly support the evaluation of the impact of land use and climate change on
71 groundwater levels and crop yields.
72

73

74

75 Keywords: groundwater recharge; capillary rise; land use; soybean; Pampas; Argentina; SWAP;
76 WOFOST

77

78		
79		
80	Contents	
81	1. Introduction	4
82	2. Method and materials	5
83	2.1. Study Area.....	5
84	2.2. Modelling Tools	6
85	2.3. Field scale.....	8
86	2.3.1. Soil physical properties	8
87	2.3.2. Parameter calibration for soybean	8
88	2.3.3. Verification of predicted soybean yields at county level	9
89	2.3.4. Parameter calibration of maize and wheat.....	9
90	2.3.5. Sensitivity analyses	9
91	2.4. Regional scale.....	9
92	2.4.1. Spatial schematization using soil, climate and land use.....	10
93	2.4.2. Soil physical parameters.....	10
94	2.4.3. Increasing groundwater levels.....	11
95	2.4.4. Land use evaluation with a crop rotation scheme and permanent grassland.....	11
96	3. Results	12
97	3.1. Field scale.....	12
98	3.1.1. Soybean calibration	12
99	3.1.2. Actual soybean at six sites compared with official statistics at county level	12
100	3.1.3. Maize and wheat.....	12
101	3.1.4. Sensitivity analysis	13
102	3.2. Regional scale.....	13
103	3.2.1. Historical situation from 1990-2015	13
104	3.2.2. Changes of groundwater levels	14
105	3.2.3. Changes of land use.....	14
106	3.2.4. Changes of land use and nitrate leaching	15
107	4. Discussion	16
108	5. Conclusions and recommendations	17
109	Acknowledgements	18
110		
111		
112		
113		

114 **1. Introduction**

115

116 Groundwater recharge results from the dynamic interaction between climate, land use and soil
117 hydrology as it occurs in the critical zone, a thin portion of the biosphere connecting the lithosphere,
118 atmosphere and hydrosphere (Amundson et al., 2007). Within this critical zone a dynamic interaction
119 occurs between soil, atmosphere and water. The variation of this interaction in space and time can be
120 very large and is influenced by human and natural activities. Especially in flat, poorly drained sub-humid
121 plains, such as the Argentine Pampas, the Brazilian Pantanal, the Canadian plains of Manitoba and
122 Saskatchewan and the Great Plains of Hungary and Western Siberia, groundwater rise may cause large
123 episodic floods (Aragón et al., 2010). This interaction has a large uncertainty which one wishes to
124 minimize, especially to predict the effects of climate change and land use on groundwater recharge
125 conditions (Smerdon, 2017). To improve the accuracy of model outputs, proper evapotranspiration data
126 as upper boundary condition and the use of remote sensing information is recommended (Doble &
127 Crosbie, 2017).

128

129 Mercau et al. (2016) analysed the impact of climate, topography and crop choice on the dynamics of
130 groundwater table levels for five years on a typical farm in the Western Pampas of Argentina. They
131 concluded that maintaining crops that increase evapotranspiration and reduce groundwater recharge for
132 long time periods this should magnify the effects of land use on the dynamics of groundwater tables.

133

134 Vazquez-Amabile et al. (2013) applied the field-scale hydrological model DrainMod (Skaggs et al.,
135 2012) at 12 farms fields within a radius of 100 km in the western Buenos Aires Province. They observed
136 groundwater table depths generally within 3 meter below the soil surface and concluded that leaching
137 of nitrate should be considered since 52% of the observations exceeded the threshold of 10 mg/L NO₃-
138 N. A significant proportion of the leached nitrate originates from mineralization of organic matter
139 (Vazquez-Amabile et al., 2017).

140

141 Viglizzo et al. (2009) found correlations between groundwater level and flooding in 12.4 million hectare
142 of the Pampas in Argentina with highly significant relations in the highlands. They also stated that land
143 use could be steered to minimize the impact of floods.

144

145 A better understanding of the underlying processes by which crops influence groundwater is essential
146 for the evaluation of different measures to influence groundwater recharge. Garcia et al. (2017) applied
147 the regional MIKE-SHE model to a sub-basin in Argentina and concluded that land use has strong effects
148 on groundwater levels. They remarked that land use decisions to control groundwater and minimize
149 negative effects on agricultural production should have a broad consensus regarding social and physical
150 aspects. The water contribution from groundwater located approximately 1.5 to 2 m deep can represent
151 up to 30% of the water requirements of soybeans in the flooding sandy Pampas, thus stabilizing the
152 inter-annual variability of soybean yields (Videla Mensegue et al., 2015). Sainato et al. (2003) reported
153 increasing salinity values in groundwater for the region around Pergamino where the aquifer shows an
154 increase in water salinity to the West.

155

156 Aragón et al. (2010) used satellite data and groundwater monitoring wells to analyse the changes of
157 groundwater depths and surface water amounts of the Western Pampas of Argentina during the flooding
158 cycle of 1996-2006. They showed that mean regional groundwater levels rose by 2.5 m in 5 years, which
159 decreased the average vadose zone from 3.7 m to 1.2 m. In the same period, the regional surface water
160 coverage (ponds, rivers, lakes) increased from 3% to 28% primarily by the development of new water
161 bodies. This had a huge impact on hydrological connectivity throughout the landscape transport and
162 flooding risks. Kuppel et al. (2015) extended the hydrologic analysis of the Pampas to the period 2000-

163 2013 and included the eastern lower part of the Pampas. They investigated three responses to periods
 164 with increased rainfall: (i) increased water storage leading to rising groundwater tables and floods, (ii)
 165 higher evapotranspiration losses favoured by higher soil moisture contents and capillary rise and, at very
 166 high levels of water storage, (iii) enhanced surface water outflows favoured by the surface water
 167 connectivity. They concluded that the first two responses are dominant: rising groundwater tables and
 168 higher evapotranspiration losses.

169
 170 A better understanding of the complex interactions between crops and shallow groundwater is therefore
 171 recommended and will help to stabilize yields and balance opportunities and risks caused by the ‘labile
 172 hydrology’ of the Pampas (Nosetto et al., 2009).

173
 174 With this paper we intend to contribute to a better understanding of the complex interactions between
 175 soil hydrology and crop growth within the critical zone. We analysed the impact of different
 176 groundwater tables and different land use types on groundwater recharge and agricultural production.
 177 An analysis of the water distribution over crops, vadose zone and groundwater is necessary to consider
 178 processes like soil moisture redistribution, root water uptake and capillary rise of groundwater. We
 179 developed a toolbox consisting of a state-of-the-art dynamic simulation model for agricultural crop
 180 growth and a Richards equation-based model for soil water flow.

181
 182 We used local observations of crop and soil parameters with special attention to a detailed determination
 183 of soil hydraulic properties. Furthermore we analysed the sensitivity of soil hydraulic parameters with
 184 respect to vertical water flow and yields. This is essential to support model and calibration improvement
 185 (De Jong van Lier et al., 2015). After calibration and evaluation we analysed the impact of changes of
 186 land use and rising groundwater level on regional agricultural production using long term climate data.
 187 This study resulted from a case study that was carried out within an EU-project and reported by De Wit
 188 et al. (2017) and Kroes et al. (2017b).

189

190 **2. Method and materials**

191 **2.1. Study Area**

192 The Pampas of Argentina cover a wide plain of about 54 million ha of fertile lands (Viglizzo et al.,
 193 2003). Based on soil and rainfall patterns, the region can be divided into different agro-ecological areas
 194 (Viglizzo et al, 2003): i) Rolling Pampas in the centre of the area, ii) Sub-humid Eastern Pampas, iii)
 195 Semiarid Western Pampas, iv) Southern Pampas, v) North-Eastern Flooding Pampas, and vi)
 196 Mesopotamian Eastern Pampas. Dominating crops are soybean and rotations of the crops maize, wheat
 197 and soybean.

198 We analysed the relation between groundwater and land use in a study area of about 40 million ha or
 199 75% of the Pampas of Argentina (Fig. 1), using a combination of a hydrological and a crop simulation
 200 model (see following sections). The grid lines indicate the boundaries of the grid cells applied in the
 201 simulation at regional scale. Within the study area we selected 6 sites for the calibration of soybean
 202 parameters; the location of these sites was based on data availability and spread over the area.

203

204 *Fig. 1. The study area and location of 6 selected sites in the Argentina Pampas. The grid lines delimit*
 205 *the grid cells applied in the simulation at regional scale.*

206

207 2.2. Modelling Tools

208 We merged different modules for crop, soil water and atmosphere and integrated the two dynamic
 209 models SWAP (acronym for Soil Water Atmosphere Plant) and WOFOST (WOrld FOod STudies).
 210 SWAP is a dynamic soil hydrological model to obtain soil water pressure head values using the Richards
 211 equation (Van Dam et al., 2008; Kroes et al., 2017a) that has been applied in many studies
 212 (<http://swap.wur.nl/References.htm>). WOFOST is a generic crop growth simulation model, of which the
 213 principles are explained by Van Keulen & Wolf (1986) and Boogaard et al. (2014). WOFOST has been
 214 applied in many studies (e.g. Supit et al., 2012; De Wit et al., 2012, Asseng et al., 2013) at different
 215 spatial scales in many regions across the world. In order to simulate the soil carbon and soil nitrogen
 216 influence, we added also the module Soil-N (Groenendijk et al., 2016).

217

218 The integrated model (Fig. 2) is distributed on internet as version 4 of the open-source model SWAP
 219 (<http://swap.wur.nl>).

220

221 *Fig. 2. Set of dynamic modelling tools integrated in SWAP version 4*

222

223 The integrated model describes a one-dimensional system that ranges from the top of the soil or
 224 vegetation, to the bottom of the unsaturated or saturated part of the relevant soil system. In this study
 225 we simulated a soil column of 5.5 m.

226 SWAP numerically solves the one-dimensional Richards equation for the unsaturated-saturated zone:

227

$$228 \frac{\partial \theta}{\partial t} = \frac{\partial}{\partial z} \left[K(h) \left(\frac{\partial h}{\partial z} + 1 \right) \right] - S_a(h) \quad (1)$$

229

230 where θ is volumetric water content ($\text{cm}^3 \text{cm}^{-3}$), t is time (d), z is the vertical coordinate (cm) taken
 231 positively upward, K is the hydraulic conductivity (cm d^{-1}), S_a is soil water extraction rate by plant roots
 232 ($\text{cm}^3 \text{cm}^{-3} \text{d}^{-1}$) and h is the soil water pressure head (cm).

233

234 To solve this equation, specified boundary conditions and soil hydraulic relations between θ , h and K
 235 are required. The upper boundary is defined by meteorological conditions which are input to the model
 236 and by a cultivation which can be a static or a dynamic type of crop (Kroes et al., 2017a). In this study
 237 we used the static sub-model for grassland and the dynamic sub-model WOFOST for both the growth
 238 of soybeans and for a crop rotation of soy-wheat-maize.

239

240 We used the Penman-Monteith method (Allen et al., 1998) to determine the potential evapotranspiration
 241 which is partitioned over potential transpiration of a crop and potential soil evaporation using the Leaf
 242 Area Index. Extensive descriptions are given in chapter 3 and appendix 1 of Kroes et al. (2017a).

243 Rainfall is input to the model as daily amounts. Runoff is calculated when the rainfall intensities
 244 supersede the soil infiltration capacity or when the soil profile becomes saturated.

245

246 The lower boundary defines the interaction with a regional groundwater flow system. The model has 5
 247 different boundary conditions which are explained in detail by Kroes et al. (2017a). In this study we
 248 applied two types of bottom boundary conditions: a) free-drainage and b) Cauchy bottom boundary
 249 condition. For the Cauchy condition, the flux through the bottom boundary (q_{bot}) is defined by the
 250 difference of the hydraulic head ($h+z$) at the column bottom and the hydraulic head ϕ (cm) of the regional
 251 groundwater below the flow domain described by the model, divided by a hydraulic resistance c (d).

252

$$253 q_{bot} = \frac{[h+z]_{z=bot} - \phi}{c} \quad (2)$$

254
255
256
257
258
259
260
261
262
263
264
265
266
267
268
269
270
271
272
273
274
275
276
277
278
279
280
281
282
283
284
285
286
287
288
289
290
291
292
293
294
295
296
297
298
299
300
301
302

We used a constant hydraulic resistance of 500 days and varied the head of the regional groundwater (ϕ) to achieve the desired average depth of the fluctuating groundwater level.

As an alternative for the commonly used soil hydraulic functions of Mualem – Van Genuchten (Mualem, 1976; Van Genuchten, 1980), the possibility to supply $\Theta(h)$ and $K(h)$ relationships as tabulated input is implemented. In that way any shape of the relationships can be considered. In this study, the tabular option is used.

The reduction of root water uptake due to too dry or too wet conditions is described according to Feddes et al. (1978). Sometimes only some parts of the root zone are stressed and show reduction of root water uptake, while other parts have favourable conditions for root water uptake. In these conditions the reduction in the stressed parts might be compensated by extra root water uptake in the parts with favourable conditions. Therefore, we extended the Feddes concept with the compensation concept of Jarvis (2011).

To simulate soybean growth, the sequential phenological development pattern in WOFOST had to be adapted. This sequential pattern is typical for cereals and is appropriate for tuber crops (potato, sugar beet), which are crops with a relative simple development pattern. For soybean a hybrid phenological development model was developed taking elements from established models for soybean phenology (Setiyono et al., 2007) but still applying the sequential development stage logic that is needed for WOFOST. Adjustments have been described in detail by De Wit et al. (2017) and were implemented in SWAP 4.

We also implemented a soil nitrogen module and used the RothC-26.3 model (Coleman et al., 1997) for an organic matter module. Both nitrogen supplied to the soil by fertilizer applications and nitrogen obtained from mineralization of organic bounded nitrogen are stored in the soil. Mineralization rates of NH_4 and NO_3 control the nitrogen mineralization and immobilization in relation to the processes in the organic matter cycle.

Ammonium and nitrate balances were calculated on a daily basis. The leaching of nitrate and ammonium was simulated to be controlled by the stock of mineral N present and the water fluxes leaching through the root zone.

The nitrogen distribution within a crop is predicted in SWAP 4 based on the method described by Shibu et al. (2010). The N-contents of crop residues are calculated in the dynamic crop module and then passed to the Soil-N module.

For soybean we assumed that a large portion of the N_2 requirement is supplied by N_2 fixation from the air. Furthermore we assume that other factors, especially phosphorus supply, are not limiting. This approach is plausible and seems in agreement with Giller (2001) who states that “*The main environmental factors that constrain N_2 -fixation in the tropics include limitations of water, nutrients (particularly phosphorus) and toxicities*”.

We assumed that 80% of the required nitrogen comes from N-fixation, a value close to the default input value of 75% mentioned by Boons-Prins et al. (1993). The remaining demand was assumed to originate from mineralisation of the organic soil matter. For soybean it implies that nutrient stress can be neglected. The adaptations for soybean and soil nitrogen in SWAP 4 have been described in detail by Groenendijk et al. (2016).

303 Using this integrated model we intended to account for different feedbacks between atmosphere, plants,
 304 soil characteristics, soil water and nitrogen limited crop growth. This allowed us to analyse in detail the
 305 impact of different land uses on groundwater recharge.
 306

307 **2.3. Field scale**

308 **2.3.1. Soil physical properties**

309 A large number of soil layers in Argentina was analysed by (Damiano 2018). He developed a
 310 pedotransfer function to obtain the soil moisture retention and hydraulic conductivity function based
 311 on soil texture data from the Argentina Pampas. The results of this analysis are the parameters of the
 312 Uni-parametric Hutson & Cass (Uni-HC) equations which was processed by Damiano (2018) to
 313 determine the soil data for 8 locations in Argentina (Table 1). The equations of the applied soil
 314 moisture retention and hydraulic conductivity functions are given by Damiano (2018).

315

316 We created input tables for the Swap model with these data and it appeared that some parameter
 317 combinations caused a discontinuity in the soil moisture retention curve near the inflection point
 318 which we adjusted by smoothing. This required an additional parameter f (Table 1) which we used to
 319 multiply the pressure head in the wet part of the soil moisture retention curve.

320

321 *Table 1. Parameters for the Argentinian soils (after Damiano, 2018) used to create the input tables.*
 322 *See Damiano (2018) for units and explanation.*

323

324 To verify the procedure we used a data set, obtained from Damiano (Damiano, 2018, personal
 325 communication) with measured values of the retention curves ($n = 78$) of the Pergamino soils (typical
 326 Argiudoll, silty loam; Soil Survey Staff, 2010). Through these data we calculated the optimal
 327 parameters of the equations presented by Damiano (2018). Results are presented in Fig. 3.

328

*Fig. 3. The curve fitted through the points of the measured water retention data of the Pergamino
 soil (left) and the correlation between the measured and computed pressure heads for a number of
 moisture contents (right).*

329

330 The left-hand part of Fig. 3 shows the fitted line and the measured soil moisture retention points. In the
 331 right-hand part of Fig. 3 the measured and computed values are plotted against each other, showing a
 332 rather good agreement.

333 **2.3.2. Parameter calibration for soybean**

334 Data for soybean field tests originated from different sites and were supplied by RECSO (Red
 335 Nacional de Evaluación de Cultivares de Soja) and UNR (National University of Rosario experiments)
 336 (De Wit et al., 2017). The observations consisted of field data from 1259 experiments over the period
 337 2011-2013 (sowing year) for five different sites: Zavalla, Venado Tuerto, Rafaela, Manfredi and La
 338 Carlotta (Table 2 and Fig. 1).

339 Calibration procedures resulted in a set of parameter for WOFOST under optimal conditions. Procedure
 340 and results are extensively described by De Wit et al. (2017). This set was applied in the integrated
 341 SWAP-WOFOST model to allow more detailed analyses of groundwater impact.

342 Since the purpose of the simulations with the integrated model had a focus on the water balance it was
 343 necessary to simulate actual yields. This required an additional calibration where we used a so-called
 344 management factor to minimize the yield gap, the difference between simulated and observed actual
 345 yields. Such a management factor accounts for pests, diseases and farm management, all of them not

346 explicitly accounted for. Our aim was to achieve a single representative value for the management factor
 347 which could then also be applied at a regional scale.

348

349

350 *Table 2 Properties of selected sites to test model results at field scale. Sites 2-6 were used for*
 351 *calibration with local field observations and for a 25 year comparison with actual yields from official*
 352 *statistics at county level.*

353 **2.3.3. Verification of predicted soybean yields at county level**

354 To verify the calibration results we simulated a longer time series using the boundary conditions from
 355 the regional simulations. Results of the 6 sites were compared with official statistics at county level for
 356 6 cases that are located in the same region as the sites with experiments (Table 2). For the 6 cases we
 357 varied sowing dates (Table 2) and we assumed a harvest date of 05-April or at maturity, whichever
 358 was earlier. Official soybean yield statistics at county level (Min. AGPA, 2016) were converted to dry
 359 matter weight, assuming an average 13% moisture content.

360 **2.3.4. Parameter calibration of maize and wheat**

361 To be able to analyse a crop rotation scheme that consisted of soybean, maize and wheat we tested
 362 maize and wheat for a long time series using official statistics at county level and meteorological data
 363 for the site San Antonio de Areco (Table 2 and Fig. 1).

364 We calibrated the maize and wheat input files. For both crops we started with default data sets for the
 365 model WOFOST7.1.7 (WofostControlCentre, 2018). We then applied artificial fertilizer (50% NH₄-N
 366 and 50% NO₃-N) at a level of 200 kg/ha N, using a fertilization scheme based on data obtained from
 367 field visits in Argentina (Table 3). We calibrated the crop parameters using official yield statistics at
 368 county level (Min. AGPA, 2016).

369

370 *Table 3 Fertilization scheme for maize and wheat.*

371 **2.3.5. Sensitivity analyses**

372 To demonstrate the interaction of input parameter on various output values, impact response surfaces
 373 (IRS) are commonly used in crop modelling (Fronzek et al., 2018). We investigated the influence of
 374 the soil physical properties of the top soil layer (20 cm) on the flux through the bottom of the root
 375 zone, which may have positive (upward) or negative (downward) values. We focused on the crop
 376 soybean because it is the predominant crop in the region and in our analysis.

377 We used the results of the calibrated soybean simulation in Zavalla, including meteorological data for
 378 four years (2011-2014). Because it was expected that groundwater depth had a large influence on the
 379 results, we performed this exercise for eight different groundwater table regimes varying from -500 to
 380 -150 cm. The influence of the soil physics of the top layer was investigated by changing saturated
 381 moisture content and saturated conductivity input values with a specified percentage. These
 382 percentages varied between -50% and +50% with 2% steps.

383

384 **2.4. Regional scale**

385 An analysis of time and space variations of actual yields and groundwater recharge was carried out
 386 using a distributed modelling approach.

387 We introduced five different groundwater conditions and three different land use types which we
 388 analysed for their impact on crop yield and groundwater recharge.

389 **2.4.1. Spatial schematization using soil, climate and land use**

390 Spatial schematization was similar to the work by De Wit et al. (2017).
 391 Overlays of maps from different gridded data sets for soil, climate and Gyga-ED zonation were made
 392 (De Wit et al., 2017). We used the detailed ISRIC WISE30sec soil map (Batjes, 2015), gridded
 393 datasets with meteorological information and a resolution of 0.25 degrees (Fig. 1). The overlays
 394 resulted in 2842 unique calculation units which were used for distributed simulations. We used the
 395 same local weather data for the 6 selected sites (Table 2) and for the distributed modelling. To
 396 evaluate the accuracy an independent evaluation set was constructed and made available by INTA
 397 (Instituto Nacional de Tecnología Agropecuaria) using daily data of 178 stations. For each station the
 398 most nearby grid cell was selected for each different data source. Minimum and maximum
 399 temperature, radiation and precipitation were included. In the vegetation and drought monitoring
 400 domain data are usually available at decadal time steps. Finally, it was decided to use different sources
 401 of meteorological data for precipitation and global radiation (De Wit et al., 2017).
 402 The rainfall amounts show large temporal differences (Fig. 4) with dry years like 1989 and 2008 that
 403 have a low median rainfall of 700 mm yr⁻¹ and wet years like 2003 and 2012 that have a median
 404 rainfall of about 1200 mm yr⁻¹. The wettest years are 2002 and 2012 with values of more than 1600
 405 mm yr⁻¹.

406
 407 *Fig. 4. Rainfall (mm yr⁻¹) in the Pampas for the years 1989 – 2015; values are given with a spatial*
 408 *variation as boxplots with median, quartile and extreme rainfall within all grids applied for the*
 409 *distributed modelling.*

410
 411 The spatial differences of rainfall are large (Fig. 5) especially in wet years 2002 and 2012. Rainfall
 412 increases from northwest to southeast.

413
 414 *Fig. 5. Rainfall (mm yr⁻¹) in the dry year 2008 (left) and in the wet year 2012 (right)*

415
 416 For the evaluation of land use changes it was assumed that all grids have a dominant land use of either
 417 soybean, a crop rotation of soybean-wheat-maize or permanent grassland.

418 **2.4.2. Soil physical parameters**

419 Hydrologic analyses usually involve the evaluation of soil water infiltration, redistribution,
 420 percolation, capillary rise and plant-water relationships. To define the hydrologic soil water effects,
 421 knowledge of soil water characteristics for water potential and hydraulic conductivity is required.
 422 Although measuring these relationships in the field or laboratory is advised to obtain the best results,
 423 these measurements are time-consuming and expensive, especially if they have to be done for a large
 424 area. Statistical correlations can be found between these soil properties and other, more easily
 425 measurable soil variables such as texture, organic matter (OM), and structure. These pedotransfer
 426 functions (ptf) can provide estimates sufficiently accurate for many regional analyses and decisions
 427 (Saxton and Rawls, 2006). For European soils the HYPRES (HYdraulic PROPERTIES of European Soils)
 428 database of pedotransfer functions (ptf's) has been developed (Wösten et al., 1999). For ptf's of soils
 429 from all over the world, another database has been created (Batjes, 2015). The main advantage of
 430 these databases is that they enable a direct link between the soil map and the soil physical
 431 characteristics. Recently, a review of the present state of ptf's has been published (Van Looy et al.,
 432 2017).

433 For Argentina Damiano (2018) developed and calibrated ptf's using local data (section .2.3.1). We
 434 applied these ptf's to generate soil physical input parameters which we used in our regional analyses.
 435 Soil texture parameters for the ptf's were taken from Batjes (2015).

436 **2.4.3. Increasing groundwater levels**

437 We simulated five different groundwater levels ranging from a depth of more than 5.5 meter to 1
 438 meter below the soil surface (Table 4). The deepest groundwater level was simulated using free
 439 drainage as bottom boundary conditions and the other four groundwater levels were simulated using a
 440 Cauchy bottom boundary condition. This condition was preferred instead of using a fixed groundwater
 441 level, because it generates more realistic fluctuations of groundwater levels and especially more
 442 realistic fluxes across the bottom boundary. This becomes especially relevant when simulating
 443 transport of several solutes simultaneously, like we did for salinity and nitrate.

444 We analysed the five different bottom boundary conditions (BBC) using a vertical hydraulic resistance
 445 of 500 days and five different regional hydraulic heads (Table 4) in the groundwater aquifer below the
 446 simulated soil column of 5.5 m.

447

448 *Table 4 Different bottom boundary conditions (BBC) applied in the regional analyses.*

449 **2.4.4. Land use evaluation with a crop rotation scheme and permanent grassland**

450 We analysed the impact of land use changes by changing the land use soybean into i) crop rotations
 451 and ii) permanent grassland. These land use changes may well be introduced in practice and occurred
 452 in past and present as was described by several authors (Viglizzo et al., 2009; Nosetto et al., 2013;
 453 Garcia et al., 2017).

454 For 3 crops (soybean, wheat and maize) used in a rotation, a preliminary test was executed to obtain
 455 realistic yields and phenology (paragraph 2.3.3 and 2.3.4). Subsequently a 25 year period was
 456 simulated using a 5-year crop rotation block consisting of the crop rotation sequence listed in Table 5
 457 and fertilizer levels the same as at field scale (Table 3). We introduced a 5-year rotation to allow an
 458 introduction of 2 types of early soybean that are characterised by different dates for sowing and
 459 harvest (Table 5).

460

461 *Table 5 A 5-year crop rotation sequence applied in the regional analyses.*

462

463 For permanent grassland we used the static modelling option, with a fixed leaf area index and rooting
 464 depth development, independent of climatic conditions and no simulation of crop yields. The leaf area
 465 index was fixed at a low value of 1.0 and the rooting depth at a value of 30 cm. With these values a
 466 low productive permanent grassland with limited transpiration is simulated.

467 We applied free-drainage as bottom boundary condition for the evaluation of land use (Table 4, BBC
 468 nr 1).

469

470 3. Results

471 3.1. Field scale

472 3.1.1. Soybean calibration

473 Observed and simulated actual yields for the site in Zavalla (Fig. 6) showed a good fit for the harvest-
 474 years 2012-2014. Calibration of the crop parameters resulted in an average potential yield of 5.9 ton
 475 ha^{-1} . There is a relatively large difference between the simulated potential and simulated actual yields.
 476 The difference between potential and attainable yield was reduced by a management factor which was
 477 manually calibrated to a value of 0.88 and resulted in an average yield reduction of 0.7 ton ha^{-1} . The
 478 management factor of 0.88 accounts for crop yield reduction processes, such as weeds, pests and
 479 diseases, which cannot be explained/described by our model. This value was regarded acceptable to
 480 explain the difference between potential and attainable yield as discussed by Van Ittersum et al.
 481 (2013), who mentioned values ranging from 0.75 to 0.85. The remaining difference between potential
 482 and actual yield was largely caused by drought during the three years. Finally a mean actual yield of
 483 3.2 ton ha^{-1} was simulated and regarded as a good result given the small difference of about 0.2 ton ha^{-1}
 484 between simulated and observed actual yields.

485

486 *Fig. 6. Results for soybean at the site Zavalla: simulated and observed harvested yield of soybeans (kg*
 487 *ha^{-1} dry matter) for the calibration years 2011-2014*

488 3.1.2. Actual soybean at six sites compared with official statistics at county level

489 We extended the simulations in space and time using 6 locations for a comparison with official
 490 statistics at county level.

491 A result for Zavalla is given in Fig. 7 showing simulated and observed yields for the period 1990-
 492 2010, a period for which statistics and model results were available. Simulated yields are higher than
 493 observed ones, indicating that we are not able to simulate all stress accurately. Our simulations for the
 494 Zavalla field neglect differences caused by variation in soil type, drainage condition and management.
 495 The statistics we used for comparison do have this variation in space and time. Given these differences
 496 in variation we think a long term yield difference of 856 kg ha^{-1} crop season⁻¹ is acceptable (Fig. 7).

497

498 *Fig. 7. Results for soybeans at the site Zavalla: Top left graph shows simulated and observed yields*
 499 *(kg ha^{-1} DM) from official statistics at county level for the period 1990-2015. Top right shows boxplot*
 500 *with median, quartile and extreme values. Lower graph shows the actual yields (kg ha^{-1} DM) during*
 501 *the period 1990-2015*

502

503 The average of simulated and observed (official statistics at county level) values show that simulated
 504 results show differences similar to the statistics. The largest statistical differences (mean error ME and
 505 root mean square error RMSE) occur for Manfredi Rafaela (Table 6).

506

507 *Table 6 Observed and simulated soybean yields (kg ha^{-1} DM): Actual and potential simulated yield*
 508 *(Y_{act} and Y_{pot}) and observed yield (Y_{obs}) and the difference between actual yield and observed yield*
 509 *(Y_{diff}) given as average values for the period 1990-2015. Simulated values result from the integrated*
 510 *model SWAP. Observations result from official statistics at county level.*

511 3.1.3. Maize and wheat

512 A result of the comparison for San Antonio de Areco for grain maize (Fig. 8a and Fig. 8b) and wheat
 513 (Fig. 8c and Fig. 8d) showed simulated and observed yields for the period 1990-2010, a period for
 514 which statistics and model results were available.

515 Resulting mean yields are within acceptable ranges. The differences within the statistical observations
 516 are larger than the differences within simulation results because the official statistics at county level
 517 include all spatial differences, while the simulations results are based on one soil type, drainage
 518 condition and management factor. Furthermore the simulated yields of both maize and wheat show
 519 much less variation than the observed yields which may also be caused by the use of one cultivar and
 520 less variation in soil types and drainage conditions than occurs within the region.

521
 522 *Fig. 8. Results for grain maize (a and b) and wheat (c and d) in San Antonio: Upper graphs show*
 523 *simulated and observed yields (kg ha⁻¹ DM) from official statistics at county level for the period 1990-*
 524 *2015. Lower graph shows boxplot with median, quartile and extreme values.*
 525

526 3.1.4. Sensitivity analysis

527 The impact of changes of hydraulic conductivity and moisture content on yield, groundwater recharge,
 528 vertical water flow to/from the root zone and runoff was analysed and results are given as IRS-charts of
 529 the yearly average values in Fig. 9. Results show that both changing conductivity and moisture content
 530 influence the resulting yield and groundwater recharge. Crop yields are especially affected by a low
 531 hydraulic conductivity and moisture content (Fig. 9a and Fig. 9b). The analyses of the effect of soil
 532 physical parameters on groundwater recharge (Fig. 9c and Fig. 9d) show a larger sensitivity for hydraulic
 533 conductivity than for saturated moisture content. A more detailed analysis will be given by Wesseling
 534 et al (in prep).

535
 536 *Fig. 9. Results of the sensitivity analysis: Impact on yield (kg ha⁻¹ yr⁻¹) of K_s and Θ_s using a*
 537 *groundwater level at an average depth of 500 cm (a) and 200 cm (b), and impact on groundwater*
 538 *recharge or bottom boundary flux (q_{bot} in mm yr⁻¹) using a groundwater level at an average depth of*
 539 *500 cm (c) and 200 cm (d).*
 540

541 3.2. Regional scale

542 3.2.1. Historical situation from 1990-2015

543 For the historical situation a soil hydrological situation with deep groundwater (>5.5 m below the soil
 544 surface) was assumed. This situation was simulated with the model SWAP using a hydrological
 545 bottom boundary condition of free-drainage (Table 4, BBC nr 1).

546
 547 The average results of the spatially distributed simulations for the period 1990-2015 show an actual
 548 soybean yield (Y_{act}) of 2.8 ton ha⁻¹ DM (Dry Matter) and an upward and downward flux across the
 549 bottom of the root zone of respectively 99 and 72 mm crop season⁻¹ (Table 7). The average downward
 550 flux across the bottom of the soil profile (groundwater recharge) is 209 mm yr⁻¹.

551
 552 The actual yields and the groundwater recharge in dry 2008 and wet 2012 are presented in Fig. 10 and
 553 Fig. 11. Soil types can be recognised in the spatial patterns of yield and groundwater recharge.

554 The groundwater recharge has relatively low median values, but shows a large spatial and temporal
 555 variation. In the wet year 2012 groundwater recharge is highest with values of more than 150 mm yr⁻¹
 556 in the soils in the NE part of the area.

557
 558 *Fig. 10. Dry year 2008: Actual yields (kg ha⁻¹ DM) (left) and groundwater recharge (mm yr⁻¹)*
 559

560 *Fig. 11. Wet year 2012: Actual yields (kg ha⁻¹ DM) (left) and groundwater recharge (mm yr⁻¹)*
 561

562 3.2.2. Changes of groundwater levels

563 Five different drainage conditions were assumed in the simulations (Table 4) which resulted in
 564 fluctuating groundwater levels at depths of more than 5 meter to 1 m below soil surface. We analysed
 565 the impact of drainage conditions on yields and groundwater recharge.

566 Actual yields of soybean generally benefit when non-saline groundwater gets closer to the root zone.

567

568 Actual soybean yields generally benefit when non-saline groundwater gets closer to the root zone. This
 569 was similarly predicted by our calculations showing a yield increase from 2.8 to 4.4 ton ha⁻¹ with
 570 increasing groundwater levels (Table 7). The upward flux to the root zone is 99 mm even in the case of
 571 free-drainage and increases to 249 mm when the groundwater level becomes shallow. This upward flux
 572 can be partitioned over a recirculation flux and capillary rise (Kroes et al., 2018). In free-drainage
 573 scenarios the upward flux is due to recirculation of percolation water and in the other scenarios with
 574 groundwater this upward flux is the sum of recirculation and capillary rise.

575

576 Simulated crop transpiration increases from 421 to 530 mm during the cultivation period due to upward
 577 water fluxes caused by capillary rise and recirculation (Table 7). The average rainfall is 928 mm yr⁻¹;
 578 runoff increases and is highest in years with shallow groundwater. As groundwater levels increase, the
 579 downward flux across the bottom of the soil profile decreases from 209 mm yr⁻¹ to an upward flux of
 580 110 mm yr⁻¹ under conditions with shallow groundwater.

581

582 The simulated flux across the root zone shows positive (upward) values (capillary rise) which
 583 increases as groundwater rises and a downward flux which is low and constant (Fig. 12). The increase
 584 is caused by the demand of the crop, which is reflected in an increasing yield as function of the
 585 upward flux across the bottom of the root zone (Fig. 13). The net flux across the bottom of the root
 586 zone increases with a rising groundwater level (Fig. 14), but the net flux across the bottom of the soil
 587 profile changes from a downward recharge to an upward extraction which will result in a lowering of
 588 the shallow groundwater (Fig. 14).

589

590 *Table 7 Simulation results for soybean: average values for the period 1990-2015. Hydraulic head as*
 591 *bottom boundary condition and average groundwater level (Gwl), actual yield (Y_{act}) and*
 592 *potential yield (Y_{pot}), actual transpiration (T_{act}), vertical flux across the bottom of the root zone*
 593 *during crop growth season, q_{RZ}^{up} is upward, q_{RZ}^{do} is downward flux, $q_{RZ}^{net} = q_{RZ}^{up} - q_{RZ}^{do}$, actual*
 594 *evapotranspiration from soil and crop (ET_{act}), and vertical flux across the bottom of the soil*
 595 *profile (q_{Bot} , positive values are upward, negative values are downward)*

596

597 *Fig. 12. Vertical water flux (q_{vert} in mm crop season⁻¹) across the lower boundary of the root zone as*
 598 *function of average groundwater level (m below soil surface); results for 5 different hydrological*
 599 *lower boundary condition; upward flux is positive, downward flux is negative*

600

601 *Fig. 13. Average actual yields (in kg ha⁻¹ DM) as function of upward water flux (mm crop season⁻¹)*
 602 *across the lower boundary of the root zone*

603

604 *Fig. 14. Vertical water flux q_{vert} (mm) across the lower boundary of the root zone (upper figure) and*
 605 *across the lower boundary of the soil profile (lower figure) as function of average groundwater table*
 606 *(m below soil surface); results for 5 different hydrological lower boundary condition; upward flux is*
 607 *positive, downward flux is negative*

608

609 3.2.3. Changes of land use

610 Three types of land use were simulated with free-drainage conditions: i) no tillage soybean, ii)
 611 rotation of maize-soybean-wheat, iii) permanent grassland.

612 The long term difference in average values of simulated groundwater recharge between crop rotation
 613 and soybean is about 1% (Table 8) which is small but has a large spatial and temporal variation with
 614 median changes of groundwater recharge that vary between 90% reduction and 55% increase.
 615 Permanent grassland reduces long term average groundwater recharge with 72% from 209 to 59 mm
 616 yr^{-1} (Table 8) and has a similar large spatial and temporal variation with median changes of
 617 groundwater recharge that vary between 94% reduction and 6% increase
 618 Both the upward and downward vertical flux across the root zone are largest under permanent
 619 grassland due to the longer growing season. The downward flux across the bottom of the root zone is
 620 highest below grassland, but the bottom flux that contributes to groundwater recharge is lowest under
 621 permanent grassland due to its large recirculation flux (Table 8).

622
 623 *Table 8 Simulation results for soybean, a crop rotation and permanent grassland: average values for*
 624 *the period 1990-2015. Free drainage as bottom boundary condition for the 3 cases. Actual yield*
 625 *(Y_{act}) and potential yield (Y_{pot}), actual transpiration (T_{act}), vertical flux across the bottom of the*
 626 *root zone during crop growth season, q_{RZ}^{up} is upward, q_{RZ}^{do} is downward flux, $q_{RZ}^{net} = q_{RZ}^{up} - q_{RZ}^{do}$,*
 627 *actual evapotranspiration from soil and crop (ET_{act}), and vertical flux across the bottom of the*
 628 *soil profile (q_{Bot} , positive values are upward, negative values are downward).*

629 3.2.4. Changes of land use and nitrate leaching

630 A comparison was made for the nitrogen leaching under free-drainage conditions with soybean and the
 631 crop rotation. Results show that the nitrate leaching below a crop rotation is about 17% higher than the
 632 nitrate leaching below soybean (Fig. 15a). Mean values of nitrate leaching for soybean and crop
 633 rotation are respectively 2.3 and 2.7 $\text{kg ha}^{-1} \text{yr}^{-1} \text{N}$. Mean values for ammonium are 0.2 and 0.3 kg ha^{-1}
 634 $\text{yr}^{-1} \text{N}$ for respectively soybean and crop rotation. Leaching of ammonium hardly occurs because, if
 635 ammonium is produced by mineralisation of organic matter, it is rapidly transformed into nitrate by
 636 nitrification. The leaching of nitrate shows a large temporal and spatial variation with a larger
 637 variation for the crop rotation (Fig. 16b) than for soybean (Fig. 16a).
 638 When one divides the leaching of nitrate-N (2.7 $\text{kg ha}^{-1} \text{yr}^{-1} \text{N}$) over the groundwater recharge (q_{Bot} in
 639 Table 8) this results in an estimated yearly average level of nitrate leaching of about 1 $\text{mg l}^{-1} \text{NO}_3\text{-N}$.
 640 However if one regards the downward leaching of water from the rootzone (66 $\text{mm crop season}^{-1}$) the
 641 leaching of nitrate has a concentration of 4.1 $\text{mg l}^{-1} \text{NO}_3\text{-N}$ which is below the drinking water standard
 642 of 10 mg l^{-1} for $\text{NO}_3\text{-N}$. In some regions higher values are found (Martinez et al., 2014) with large
 643 differences in space and time (Aparicio et al., 2008).

644
 645 *Fig. 15. Boxplots with results of downward leaching flux ($\text{kg ha}^{-1} \text{yr}^{-1} \text{N}$) of $\text{NO}_3\text{-N}$ (a) and $\text{NH}_4\text{-N}$ (b)*
 646 *across bottom of soil profile below crop rotation (left) and soybean (right) under free-drainage*
 647 *conditions.*

648
 649 *Fig. 16. Boxplots with results of downward leaching flux $\text{NO}_3\text{-N}$ ($\text{kg ha}^{-1} \text{yr}^{-1} \text{N}$) across bottom of soil*
 650 *profile below soybean (a) and crop rotation (b).*

651

652 4. Discussion

653

654 Results for actual yields show a large variation for field sites within a region. Aramburu Merlos et al.
 655 (2015) estimated actual yields for a larger part of Argentina to be 2.65 ton ha⁻¹, based on statistics. We
 656 simulated actual yields of 2.79 ton ha⁻¹ DM (Table 7). The relatively small difference can be caused by
 657 many reasons, such as other groundwater level fluctuations, a different soybean variety or a poor
 658 estimate of the management impact .

659

660 The calculated soybean evapotranspiration shows a good agreement with results from Nosetto et al.
 661 (2012) who determined 670 mm yr⁻¹ which is close to the 692 mm yr⁻¹ we calculated (Table 8) as long
 662 term average for a larger area and a long time series.

663

664 In order to lower groundwater levels and reduce the risk of flooding, groundwater recharge should be
 665 reduced. A minor reduction will be achieved by changing from monoculture soybean to crop rotations
 666 and a larger change will be achieved by changing to other types of land use like permanent grassland
 667 or trees. These land use systems will decrease groundwater recharge and contribute to lowering of
 668 groundwater levels.

669 The recommendation for grassland and trees is in agreement with a study by Nosetto et al. (2012) who
 670 determined, for a region just north of our study region, high evapotranspiration of 1100 mm yr⁻¹ for
 671 native forest and eucalyptus plantations compared to 670-800 mm yr⁻¹ for herbaceous canopies.

672

673 Mercau et al. (2016) explored the impact of different crops on groundwater levels and concluded that
 674 crops do not have a substantial effect on the longer term dynamics of the water table. High groundwater
 675 levels offer an opportunity which should be carefully considered. It increases capillary rise, allows a
 676 more intensive use of irrigation and a higher variety of crops. Frequent on-farm and regional monitoring
 677 of groundwater levels should support cultivation strategies.

678

679 The simulations showed the sensitivity of yields, evapotranspiration and groundwater recharge for soil
 680 physical parameters. Soil physical properties play an important role in the distribution of the
 681 precipitation excess. We applied the ISRIC WISE30sec soil map (Batjes, 2015) with world soil property
 682 estimates and used it to transform soil texture into model parameters using so-called pedo-transfer (ptf)
 683 functions. Several datasets are available for different scales. Montzka et al. (2017) describe a global
 684 dataset based on ROSETTA (Schaap et al., 2001) applied to the SoilGrids1km data set of Hengl et al.
 685 (2014). Van Looy et al. (2007) give an overview of ptf's and recommend not to use ptf's beyond the
 686 region or soil type from which it was developed. The soils of the Pampas are very atypical, therefore
 687 we refined the parameterisation using local and regional datasets. We used the ISRIC soil map in
 688 combination with local soil physical data from Damiano (2018). Further improvements can be achieved
 689 using more local soil information.

690

691 Long term NT (No Tillage) of soybean cultivation may cause a platy structure of soils in the Argentina
 692 Pampas (Sasal et al, 2017a and 2017b) which will have impact on the partitioning of the precipitation
 693 excess over surface and subsurface runoff and groundwater recharge. This impact is mainly caused by
 694 a rooting depth reduction due to the poor permeability of the platy structured soils. We used a model
 695 experiment for the Zavalla site where we varied the maximum rooting depth to quantify the impact of
 696 platy soil structure on yield and groundwater recharge. Results show that the actual yields may be
 697 reduced from about 2.7 to 1.7 ton ha⁻¹ DM and the groundwater recharge may increase from 246 to
 698 331 mm (Fig. 17).

699

700

701 *Fig. 17. Results of limited rooting depth on actual yield and on groundwater recharge q_{Bot} .*
 702 *Actual yield (kg ha^{-1} DM) and groundwater recharge as flux across bottom of soil profile ($q_{Bot} = q_{vert}$*
 703 *in mm yr^{-1}) as function of maximum rooting depth (cm).*

704
 705 Lowering groundwater without irrigation causes drought and successive crop and yield damage. In the
 706 Pampas of Argentina irrigation is marginal. However, rising groundwater may offers more
 707 opportunities for irrigation which may increase, contribute to increased evapotranspiration and, as a
 708 consequence, lower the groundwater again.

709
 710 Salinity is an important issue when saline groundwater rises above critical levels (Nosetto et al.
 711 (2013). Salinity control measures were evaluated for the Mendoza area by Kupper et al. (2002) who
 712 applied the regional hydrological model SIMGRO and concluded that using more groundwater is an
 713 effective measure to control salinity in the root zone.

714 We carried out a regional scale analyses with a salinity level of 3 g l^{-1} in the upward seepage water
 715 flux across the bottom boundary for situations with average groundwater levels at 2 and 1 meter below
 716 the soil surface. Results showed a very low impact on soybean yields. However, this is not
 717 representative for the relation between land use and salinization which should be analysed in a broader
 718 perspective (Nosetto et al., 2013) because for more salt-sensitive types of land use an increase of
 719 salinity may have a large impact.

720
 721 The use of remote sensing was limited in this study, but future developments will facilitate the
 722 increase of its use. Land use maps at field scale level like crop type (needed for rotations) are not easy
 723 to obtain for Argentina. New procedures are being developed at INTA to generate new land use maps
 724 and facilitate the choice of meteorological data.

725 This study does not account for all features that influence groundwater recharge. The impact of
 726 geological controls in subsoils, impact of steep slopes and processes like ponding are only partially
 727 covered and can definitely be improved.

728
 729 A regional analysis with real-time observations of groundwater levels was beyond the scope of this
 730 study. However, several monitoring sites exist (Aragón et al., 2010; Kuppel et al., 2015) and
 731 intensification is under way. This may support early warning systems (Viglizzo et al., 2009) and
 732 enable a regional study using realistic groundwater levels as bottom boundary or as calibration in
 733 future studies.

734
 735 Opportunities are created when a proper balance is found between supply and demand of soil water
 736 using a larger differentiation of land use. Increasing the areas of land use types with higher
 737 evapotranspiration, like permanent grassland and trees, will contribute to a more stable hydrologic
 738 system with more water storage capacities in the soil system and lower groundwater levels.

739 **5. Conclusions and recommendations**

740 Based on several modelling exercises the findings can be summarized as:

- 741 • Groundwater recharge from the unsaturated zone and from the root zone shows large differences
 742 and should be analysed separately;
- 743 • Rising groundwater has an impact on agricultural production with large spatial and temporal
 744 differences;
- 745 • Rising groundwater may reduce groundwater recharge (negative feedback);
- 746 • Crop rotations may increase the risk of nitrogen leaching when compared to monoculture no-
 747 tillage soybean;

- 748 • Multi-crop rotations may decrease groundwater recharge when compared to monoculture no-
749 tillage soybean;
- 750 • Platy soil structure under no-tillage soybean reduces yields and increases groundwater recharge;
- 751 • Increasing the areas of land use types with higher evapotranspiration, like permanent grassland
752 and trees, will contribute to a more stable hydrologic system with more water storage capacities in
753 the soil system and lower groundwater levels;
- 754 • Monitoring of groundwater levels at field and regional scale should be intensified to support early
755 warnings systems and future studies;
- 756 • Model analyses support the search to find a proper balance between positive and negative impacts
757 of land use changes.

758
759
760
761

762 **Acknowledgements**

763 We thank contributions from the projects SIGMA (Stimulating Innovation for Global Monitoring of
764 Agriculture, grant agreement No. 603719) and WaterVision Agriculture (www.waterwijzer.nl, project
765 KB-14-001-046). Lucas Borrás and José Rotundo provided key knowledge on cropping practices as
766 well as soybean data from yield field trials performed at Facultad de Ciencias Agrarias, Zavalla –
767 Universidad Nacional de Rosario. We thank Marcelo Nosetto for valuable discussions on groundwater
768 dynamics in the Pampas.

Agrohydrological analysis of groundwater recharge and land use changes in the Pampas of Argentina

Joop Kroes, Jos van Dam, Iwan Supit, Diego de Abelleira, Santiago Verón, Allard de Wit, Hendrik Boogaard, Marcos Angelini, Francisco Damiano, Piet Groenendijk, Jan Wesseling, Ab Veldhuizen

Contents

References	1
Tables	6
Figures	9

References

- Allen, R.G., Pereira, L.S., Raes, D., Smith, M., 1998. Crop evapotranspiration. Guidelines for computing crop water requirements. Irrigation and Drainage Paper 56, FAO, Rome, Italy, 300 p. Retrieved from <http://www.fao.org/docrep/X0490E/X0490E00.htm>, accessed on 7 May 2018.
- Amundson, R., Richter, D.D., Humphreys, G.S., Jobbágy, E.G., Gaillardet, J., 2007. Coupling between biota and earth materials in the critical zone. *Elements*, 3(5), 327–332. <http://doi.org/10.2113/gselements.3.5.327>
- Aparicio, V., Costa, J.L., Zamora, M., 2008. Nitrate leaching assessment in a long-term experiment under supplementary irrigation in humid Argentina. *Agricultural Water Management*, 95(12), 1361–1372. <http://doi.org/10.1016/j.agwat.2008.06.003>
- Aragón, R., Jobbágy, E.G., Viglizzo, E.F., 2010. Surface and groundwater dynamics in the sedimentary plains of the Western Pampas (Argentina). *Ecohydrology*, 4(3), 433–447.
- Aramburu Merlos, F., Monzon, J.P., Mercau, J.L., Taboada, M., Andrade, F.H., Hall, A.J., Jobaggy, E., Cassman, K.G., Grassini, P., 2015. Potential for crop production increase in Argentina through closure of existing yield gaps. *Field Crops Research*, 184, 145–154. <http://doi.org/10.1016/j.fcr.2015.10.001>.
- Asseng, S., Ewert, F., Rosenzweig, C., Jones, J.W., Hatfield, J.L., Ruane, A.C., Boote, K.J., Thorburn, P.J., Rötter, R.P., Cammarano, D., Brisson, N., Basso, B., Martre, P., Aggarwal, P.K., Angulo, C., Bertuzzi, P., Biernath, C., Challinor, A.J., Doltra, J., Gayler, S., Goldberg, R., Grant, R., Heng, L., Hooker, J., Hunt, L.A., Ingwersen, J., Izaurralde, R.C., Kersebaum, K.C., Müller, C., Naresh Kumar, S., Nendel, C., O’Leary, G., Olesen, J.E., Osborne, T.M., Palosuo, T., Priesack, E., Ripoche, D., Semenov, M.A., Shcherbak, I., Steduto, P., Stöckle, C., Stratonovitch, P., Streck, T., Supit, I., Tao, F., Travasso, M., Waha, K., Wallach, D., White, J.W., Williams, J.R., Wolf, J., 2013. Uncertainty in simulating wheat yields under climate change. *Nature Climate Change*, (June). 1–6. <https://doi.org/10.1038/ncliante1916>
- Batjes, N.H., 2015. World soil property estimates for broad- scale modelling (WISE30sec). *ISRIC Report 2015/01*. Belmans, C., Wesseling JG, Feddes RA, 1983. Simulation of the water balance of a cropped soil: SWATRE. *J. Hydrol.*, 63, 271-286.
- Boogaard, H.L., Van Diepen, C.A., Rötter, R.P., Cabrera, J.M.C., Van Laar, H.H., 2014. WOFOST Control Centre 2.1 and WOFOST 7.1.7 - User’s guide for the WOFOST CONTROL CENTRE 2.1 and the crop growth simulation model WOFOST 7.1.7. Available at <https://www.wur.nl/en/Research-Results/Research-Institutes/Environmental-Research/Facilities-Products/Software-and-modelsWENR/WOFOST/Documentation-WOFOST.htm> accessed last on 21 May 2018.

- Boons-Prins, E.R., de Koning, G.H., van Diepen, C.A., Penning de Vries, F.W.T., 1993. Crop-specific simulation parameters for yield forecasting across the European Community. Reports CABO-TT, no 32.
- Coleman, K., Jenkinson, D.S., Crocker, G.J., Grace, P.R., Klir, J., Korschens, M., Poulton, P.R., Richter, D.D., 1997. Simulating trends in soil organic carbon in long-term experiments using RothC-26.3. *Geoderma*, 81(1-2), 5–28.
- Damiano, F., 2018. Modelización de parámetros hidráulicos del suelo en una cuenca hidrográfica de la región pampeana. *Journal of Soil Science, AACCS, Argentina*. In press
- De Jong van Lier, Q., Wendroth, O., van Dam, J.C., 2015. Prediction of winter wheat yield with the SWAP model using pedotransfer functions: an evaluation of sensitivity, parameterization and prediction accuracy. *Agricultural Water Management*, 154, 29-42.
- De Wit, A.J.W., Duveiller, G., Defourny, P., 2012. Estimating regional winter wheat yield with WOFOST through the assimilation of green area index retrieved from MODIS observations. *Agricultural and Forest Meteorology*, 164: 39-52.
- De Wit, A., Abelleira, D., Veron, S., Kroes, J., Supit, I., Boogaard, H., 2017. *Technical description of crop model (WOFOST) calibration and simulation activities for Argentina, pampas region*. EU-SIGMA report WP4.
- Doble, R.C., Crosbie, R.S., 2017. Review: Current and emerging methods for catchment-scale modelling of recharge and evapotranspiration from shallow groundwater. *Hydrogeology Journal*, 25(1), 3–23.
- Feddes, R.A., Kowalik, P.J., Zaradny, H., 1978. Simulation of field water use and crop yield. Simulation Monographs. Pudoc. Wageningen. 189 pp. Available at <http://edepot.wur.nl/168026> accessed last on 19 May 2018.
- Fronzek, S., Pirttioja, N., Carter, T.R., Bindi, M., Hoffmann, H., Palosuo, T., Ruiz-Ramos, M., Tao, F., Trnka, M., Acutis, M., Asseng, S., Baranowski, P., Basso, B., Bodin, P., Buis, S., Cammarano, D., Deligios, P., Destain, M., Dumont, B., Ewert, F., Ferrise, R., François L., Gaiser, T., Hlavinka, P., Jacquemin, I., Kersebaum, K.C., Kollas, C., Krzyszczak, J., Lorite, I.J., Minet, J., Ines M., Montesino, M., Moriondo, M., Müller, C., Nendel, C., Öztürk, I., Perego, A., Rodríguez, A., Ruane, A.C., Ruget, F., Sanna, M., Semenov, M.A., Slawinski, C., Pierre Stratonovitch, P., Iwan Supit, I., Waha, K., Wang, E., Wu, L., Zhao, Z., 2018. Classifying multi-model wheat yield impact response surfaces showing sensitivity to temperature and precipitation change. *Agricultural Systems*, 159, 209–224. <http://doi.org/10.1016/j.agsy.2017.08.004>
- García, Pablo E., Menéndez, Angel N., Podestá Guillermo, Bert, Federico, Arora, Poonam, Jobbágy, Esteban, 2017. Land use as possible strategy for managing water table depth in flat basins with shallow groundwater, *International Journal of River Basin Management*, 16:1, 79-92
- Giller, K.E., 2001. Nitrogen fixation in tropical cropping systems. 2nd Edition. CABI Publishing. Field Crops Research (Vol. 34). CABI Publishing. [http://doi.org/10.1016/0378-4290\(93\)90012-C](http://doi.org/10.1016/0378-4290(93)90012-C)
- Groenendijk, P., Boogaard, H., Heinen, M., Kroes, J., Supit, I., Wit, A. De., 2016. Simulation of nitrogen-limited crop growth with SWAP / WOFOST. *Report 2721. Alterra Rapport*, 2721.
- Hengl, T., de Jesus, J.M., MacMillan, R.A., Batjes, N.H., Heuvelink, G.B.M., Ribeiro, E., Samul-Rosa, A., Kempen, B., Leenaars, J.G.B., Walsh, M.G., Gonzalez, M.R., 2014. SoilGrids1km - Global Soil Information Based on Automated Mapping. *PloS One*, 9.
- Jarvis, N.J., 2011. Simple physics-based models of compensatory plant water uptake: concepts and eco-hydrological consequences. *Hydrology and Earth System Sciences*, 15(11), 3431–3446. <http://doi.org/10.5194/hess-15-3431-2011>.
- Kroes, J.G., Van Dam, J.C., Bartholomeus, R.P., Groenendijk, P., Heinen, M., Hendriks, R.F.A., Mulder, H.M., Supit, I., Van Walsum, P.E.V., 2017a. SWAP version 4, Theory description and user manual. Wageningen Environmental Research, ESG Report 2780. <http://library.wur.nl/WebQuery/wurpubs/fulltext/416321>, accessed on 7 May, 2018

- Kroes, J.G., Groenendijk, P., Abelleira, D. de, Verón, S.R., Plotnikov, D., Bartalev, S., Yan, N, Wu, B., Kussul, N., Fritz, S, 2017b. Environmental Impact Assessment of Agricultural Land Use Changes. EU-SIGMA report WP5.1. version 2.0. <https://library.wur.nl/WebQuery/wurpubs/fulltext/445875>
- Kroes, J., Supit, I., Van Dam, J., Van Walsum, P., Mulder, M., 2018. Impact of capillary rise and recirculation on simulated crop yields. *Hydrol. Earth Syst. Sci.*, 22, 2937-2951. <https://doi.org/10.5194/hess-22-2937-2018>
- Kuppel, S., Houspanossian, J., Noretto, M.D., Jobbágy, E.G, 2015. What does it take to flood the Pampas?: Lessons from a decade of strong hydrological fluctuations. *Water Resour. Res.*, 51(4), 2937-2950
- Kupper, E., Querner, E.P., Morábito, J.A., Menenti, M., 2002. Using the SIMGRO regional hydrological model to evaluate salinity control measures in an irrigation area. *Agricultural Water Management*, 56(1), 1–15.
- Martínez, D., Moschione, E., Bocanegra, E., Glok Galli, M., Aravena, R., 2014. Distribution and origin of nitrate in groundwater in an urban and suburban aquifer in Mar del Plata, Argentina. *Environmental Earth Sciences*, 72(6), 1877–1886. <http://doi.org/10.1007/s12665-014-3096-x>
- Mercau, J.L., Noretto, M.D., Bert, F., Giménez, R., Jobbágy, E.G., 2016. Shallow groundwater dynamics in the Pampas: Climate, landscape and crop choice effects. *Agricultural Water Management*, 163, 159–168.
- Min. AGPA, 2016. Ministerio de Agricultura Ganaderia Pesca y Alimentacion - Estimaciones Agrícolas (http://www.siia.gov.ar/sst_pcias/estima/estima.php , accessed on 4-Oct-2016)
- Montzka, C., Herbst, M., Weihermüller, L., Verhoef, A., Vereecken, H., 2017. A global data set of soil hydraulic properties and sub-grid variability of soil water retention and hydraulic conductivity curves. *Earth System Science Data Discussions*, 1–25
- Mualem, Y., 1976. A new model for predicting the hydraulic conductivity of unsaturated porous media. *Water Resour. Res.*, 12, 513-522.
- Noretto, M.D., Jobbágy, E.G., Jackson, R.B., Sznaider, G.A., 2009. Reciprocal influence of crops and shallow ground water in sandy landscapes of the Inland Pampas. *Field Crops Research*, 113(2), 138–148.
- Noretto, M.D., Jobbágy, E.G., Brizuela, A.B., Jackson, R.B., 2012. The hydrologic consequences of land cover change in central Argentina. *Agriculture, Ecosystems and Environment*, 154, 2–11.
- Noretto, M.D., Acosta, A.M., Jayawickreme, D.H., Ballesteros, S.I., Jackson, R.B., Jobbágy, E.G., 2013. Land-use and topography shape soil and groundwater salinity in central Argentina. *Agricultural Water Management*, 129, 120–129.
- Sainato, C., Galindo, G., Pomposiello, C., Malleville, H., de Abelleira, D., Losinno, B., 2003. Electrical conductivity and depth of groundwater at the Pergamino zone (Buenos Aires Province, Argentina) through vertical electrical soundings and geostatistical analysis. *Journal of South American Earth Sciences*, 16(2), 177–186.
- Sasal, M.C., Léonard, J., Andriulo, A., Boizard, H., 2017a. A contribution to understanding the origin of platy structure in silty soils under no tillage. *Soil and Tillage Research*, 173, 42–48.
- Sasal, M.C., Boizard, H., Andriulo, A.E., Wilson, M.G., Léonard, J, 2017b. Platy structure development under no-tillage in the northern humid Pampas of Argentina and its impact on runoff. *Soil and Tillage Research*, 173, 33–41.
- Saxton, K., Rawls, W., 2006. Soil Water Characteristic Estimates by Texture and Organic Matter for Hydrologic Solutions. *Soil Science Society of America Journal*, 70, 1569–1578.
- Schaap, M.G., Leij, F.J., Van Genuchten, M.T., 2001. Rosetta: a computer program for estimating soil hydraulic parameters with hierarchical pedotransfer functions. *Journal of Hydrology*, 251, 163–176.

- Setiyono, T.D., Weiss, A., Specht, J., Bastidas, A.M., Cassman, K.G., Dobermann, A., 2007. Understanding and modeling the effect of temperature and daylength on soybean phenology under high-yield conditions. *Field Crops Research*, 100(2–3), 257–271.
- Shibu, M.E., Leffelaar, P.A., van Keulen, H., Aggarwal, P.K., 2010. LINTUL3, a simulation model for nitrogen-limited situations: Application to rice. *European Journal of Agronomy*, 32(4), 255–271. <http://doi.org/10.1016/j.eja.2010.01.003>
- Skaggs, R.W., Youssef, M.A., Chescheir, G.M., 2012. Drainmod: model use, calibration and validation. *Transactions of the ASABE*, 55(4), 1509–1522.
- Smerdon, B.D., 2017. A synopsis of climate change effects on groundwater recharge. *Journal of Hydrology*, 555, 125–128
- Soil Survey Staff, 2010. Claves para la Taxonomía de suelos. USDA, Dpto de Agricultura USA. Traducción, Ortiz, C & MC Gutiérrez. 331p.
- Supit, I., van Diepen, C.A., de Wit, A.J.W., Wolf, J., Kabat, P., Baruth, B., Ludwig, F., 2012. Assessing climate change effects on European crop yields using the Crop Growth Monitoring System and a weather generator. *Agricultural and Forest Meteorology*, 164, 96–111.
- Van Dam, J.C., Groenendijk, P., Hendriks, R.F.A., Kroes, J.G., 2008. Advances of Modeling Water Flow in Variably Saturated Soils with SWAP. *Vadose Zone Journal*, 7(2), 640–653. <http://doi.org/10.2136/vzj2007.0060>
- Van Genuchten, M.Th., 1980. A closed form equation for predicting the hydraulic conductivity of unsaturated soils. *Soil Sci. Soc. Am. J.*, 44, 892–898.
- Van Ittersum, M.K., Cassman, K.G., Grassini, P., Wolf, J., Tittonell, P., Hochman, Z., 2013. Yield gap analysis with local to global relevance-A review. *Field Crops Research*, 143, 4–17.
- Van Keulen, H., Wolf, J., (Eds), 1986. Modelling of agricultural production: weather, soils and crops. Simulation Monographs, Pudoc Wageningen, the Netherlands, 479p. Available at <https://edepot.wur.nl/168025> accessed on 17 May 2018.
- Van Looy, K., Bouma, J., Herbst, M., Koestel, J., Minasny, B., Mishra, U., Montzka, C., Nemes, A., Pachepsky, Y., Padarian, J., Schaap, M., Tóth, B., Verhoef, A., Vanderborght, J., van der Ploeg, M., Weihermüller, L., Zacharias, S., Zhang, Y., Vereecken, H., 2017. Pedotransfer functions in Earth system science: challenges and perspectives. *Reviews of Geophysics*, 1–58.
- Vázquez-Amabile, G., Bosch, N., Ricca, A.P., Ortiz-de-Zarate, M.L., Rojas, D., Lascombes, J., Parra, V., Duarte, G., Feiguin, M.F., 2013. Evaluation of DRAINMOD model to study groundwater table dynamics and N load in Western Pampas, Argentina. *American Society of Agricultural and Biological Engineers Annual International Meeting 2013, ASABE 2013*, 3(131595082), 0–13.
- Vázquez-Amabile, G.G., Bosch, N., Ricca, A.P., Rojas, D.E., Zárate, M.L.O. De, Lascombes, J., Feiguin, M.F., Cristos, D., 2017. Napa freática: dinámica, variables de control y contenido de nitratos en suelos de pampa arenosa. *Ciencia Del Suelo*, 35(1041), 117–134.
- Videla Mensegue, H., Degioanni, A., Cisneros, J, 2015. Estimating shallow water table contribution to soybean water use in Argentina. *Eur. Sci. J.*, 11(14), 23–40.
- Viglizzo, E.F., Pordomingo, A.J., Castro, M.G., Lertora, F.A., 2003. Environmental assessment of agriculture at a regional scale in the Pampas of Argentina, 2003.
- Viglizzo, E.F., Jobbagy, E.G., Carreño, L.V., Frank, F.C., Aragón, R., De Oro, L., Salvador, V.S, 2009. The dynamics of cultivation and floods in arable lands of central Argentina. *Hydrology and Earth System Sciences Discussions*, 5(4), 2319–2345.
- Wesseling, J.G., Kroes, J.G., Campos Oliveira, T., Damiano, F., in prep. Sensitivity and uncertainty analyses of models: much easier than expected!. Paper submitted to the 2nd International Soil Modelling Conference, 5-7 November 2018, Wageningen

- WofostControlCentre, 2018. WOFOST Control Centre, available at <https://www.wur.nl/en/Expertise-Services/Research-Institutes/Environmental-Research/Facilities-Products/Software-and-models/WOFOST/Downloads-WOFOST.htm> , last access on 14 May 2018.
- Wösten, J.H.M., Lilly, A., Nemes, A., Bas, C. Le, 1999. Development and use of a database of hydraulic properties of European soils. *Geoderma*, **90**, 169–185.

Tables

Table 1 Parameters for the Argentinian soils (after Damiano, 2018) used to create the input tables. See Damiano (2018) for units and explanation.

Code	Location	b	PSI _e (ψ_e)	PSI _i (ψ_i)	Theta (θ_i)	D	K_s	f
Ar	Arrecifes	6.94	10.8	17.5	0.451	0.026	0.045	0.849
AD	Arroyo Dulce	6.98	11.0	17.9	0.449	0.027	0.046	0.872
Go	Gouin	7.52	13.3	21.5	0.472	0.024	0.045	0.959
Pe	Pergamino	7.52	14.6	23.7	0.456	0.024	0.058	0.874
Ra	Ramallo	7.75	16.8	27.2	0.462	0.023	0.026	0.860
Ro	Rojas	7.38	15.7	25.5	0.435	0.025	0.081	0.759
SL	Santa Lucia	7.61	14.4	23.4	0.467	0.024	0.037	0.938
VT	Venado Tuerto	7.42	13.1	21.3	0.446	0.024	0.063	0.914

Table 2 Properties of selected sites to test model results at field scale. Site 2-6 were used for calibration with local field observations and for a 25 year comparison with actual yields from official statistics at county level.

Site Nr	Site Name	Meteo station	Longitude	Latitude	CaseNr	Sowing date
1	San Antonio de Areco	San Antonio de Areco	-59.58	-34.23	2317	1-nov
2	Zavalla	Zavalla UNR WS	-60.88	-33.02	1626	14-nov
3	VenadoTuerto	Venado Tuerto Aero	-61.95	-33.75	2030	14-nov
4	Rafaela	Rafaela INTA WS	-61.55	-31.18	806	24-nov
5	Manfredi	Manfredi INTA WS	-63.77	-31.82	1000	14-nov
6	La Carlota	Rio Cuarto Aero WS	-64.23	-33.12	1881	14-nov

Table 3 Fertilization scheme for maize and wheat.

Crop	Date of application	Dosage (kg ha ⁻¹)
Maize	03 October	50
Maize	15 November	150
Wheat	01 June	125
Wheat	01 August	75

Table 4 Different bottom boundary conditions (BBC) applied in the regional analyses.

BBC nr	Regional groundwater head (m below soil surface)
1	>5.5 (Free drainage)
2	4
3	3
4	2
5	1

Table 5 A 5-year crop rotation sequence applied in the regional analyses.

Crop	Date Sowing	Date Harvest
Maize	01 October year 1	15 April year 2
Early Soybean	01 November year 2	25 April year 3
Wheat	01 July year 3	30 November year 3
Late Soybean	01 December year 3	01 August year 4
Maize	01 October year 4	15 April year 5
Early Soybean	01 October year 5	15 April year 6

Table 6 Observed and simulated soybean yields (kg ha^{-1} DM); Actual and potential simulated yield (Y_{act} en Y_{pot}) and observed yield (Y_{obs}) and the difference between actual yield and observed yield (Y_{diff}) given as average values for the period 1990-2015. Simulated values result from the integrated model SWAP. Observations result from official statistics at county level.

Location	Y_{pot}	Y_{act}	Y_{obs}	Y_{diff}
1_SanAntonio	5813	3064	2408	656
2_Zavalla	5853	3265	2408	856
3_VenadoTuerto	5907	2775	2537	238
4_Rafaela	5527	3185	2264	921
5_Manfredi	5799	3164	2003	1161
6_LaCarlota	5874	2659	1908	751
Average 1-6	2255	3019	764	764

Table 7 Simulation results for soybean: average values for the period 1990-2015. Hydraulic head as bottom boundary condition and average groundwater level (Gwl), actual yield (Y_{act}) and potential yield (Y_{pot}), actual transpiration (T_{act}), vertical flux across the bottom of the root zone during crop growth season, q_{RZ}^{up} is upward, q_{RZ}^{do} is downward flux, $q_{RZ}^{net} = q_{RZ}^{up} - q_{RZ}^{do}$, actual evapotranspiration from soil and crop (ET_{act}), and vertical flux across the bottom of the soil profile (q_{Bot} , positive values are upward, negative values are downward).

hydraulic head	Gwl	Y_{act}	Y_{pot}	T_{act}	q_{RZ}^{up}	q_{RZ}^{do}	q_{RZ}^{net}	Rain	Runoff	ET_{act}	q_{Bot}
m- soil surface	m-soil surface	kg ha^{-1} DM	kg ha^{-1} DM	mm season ⁻¹	mm season ⁻¹	mm season ⁻¹	mm season ⁻¹	mm yr ⁻¹	mm yr ⁻¹	mm yr ⁻¹	mm yr ⁻¹
>5.5	6	2792	5753	421	99	72	27	928	18	692	-209
4	4	3127	5753	447	125	73	52	928	22	719	-180
3	3	3567	5753	479	159	74	85	928	34	755	-132
2	2	4085	5753	513	205	73	132	928	74	809	-41
1	1	4435	5753	530	248	60	188	928	163	871	110

Table 8 Simulation results for soybean, a crop rotation and permanent grassland: average values for the period 1990-2015. Free drainage as bottom boundary condition for the 3 cases. Actual yield (Y_{act}) and potential yield (Y_{pot}), actual transpiration (T_{act}), vertical flux across the bottom of the root zone during crop growth season, q_{RZ}^{up} is upward, q_{RZ}^{do} is downward flux, $q_{RZ}^{net} = q_{RZ}^{up} - q_{RZ}^{do}$, actual evapotranspiration from soil and crop (ET_{act}), and vertical flux across the bottom of the soil profile (q_{Bot} , positive values are upward, negative values are downward).

Case Description	Y_{act}	Y_{pot}	T_{act}	q_{RZ}^{up}	q_{RZ}^{do}	q_{RZ}^{net}	Rain	Runoff	ET_{act}	q_{Bot}
	kg ha ⁻¹ DM	kg ha ⁻¹ DM	mm season ⁻¹	mm season ⁻¹	mm season ⁻¹	mm season ⁻¹	mm yr ⁻¹	mm yr ⁻¹	mm yr ⁻¹	mm yr ⁻¹
soybean	2792	5753	421	99	72	27	928	18	692	-209
crop rotation	2878	7439	345	70	66	5	924	17	695	-206
grassland			599	168	215	-47	924	20	832	-59

Figures

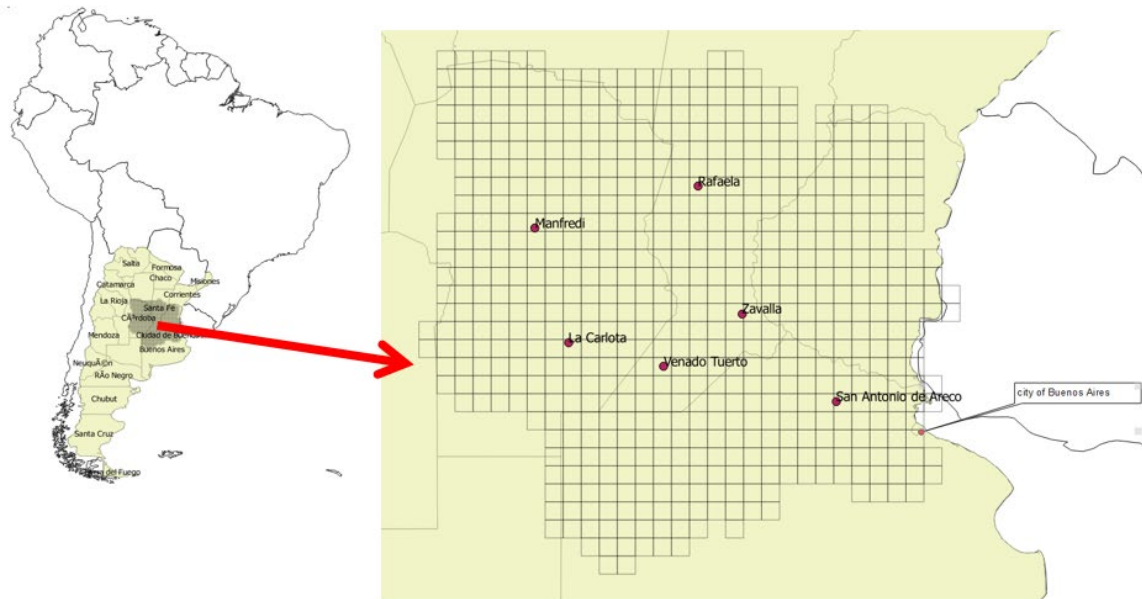


Fig. 1. The study area and location of 6 selected sites in the Argentina Pampas. The grid lines delimit the grid cells applied in the simulation at regional scale

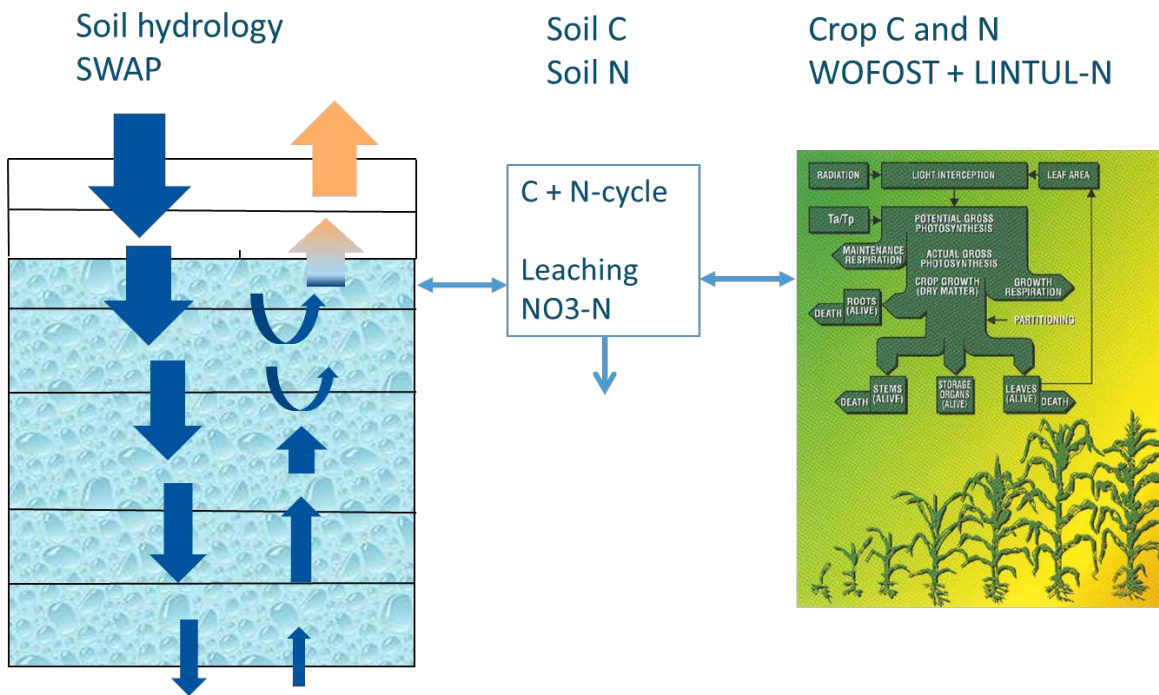


Fig. 2. Set of dynamic modelling tools integrated in SWAP version 4

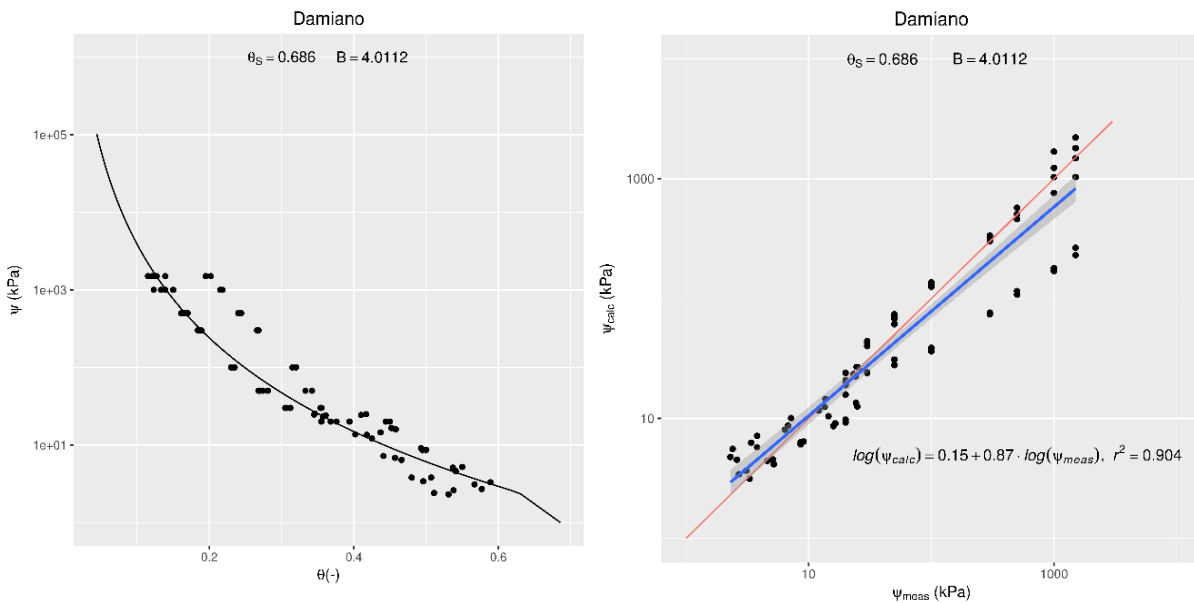


Fig. 3. The curve fitted through the points of the measured water retention data of the Pergamino soil (left) and the correlation between the measured and computed pressure heads for a number of moisture contents (right).

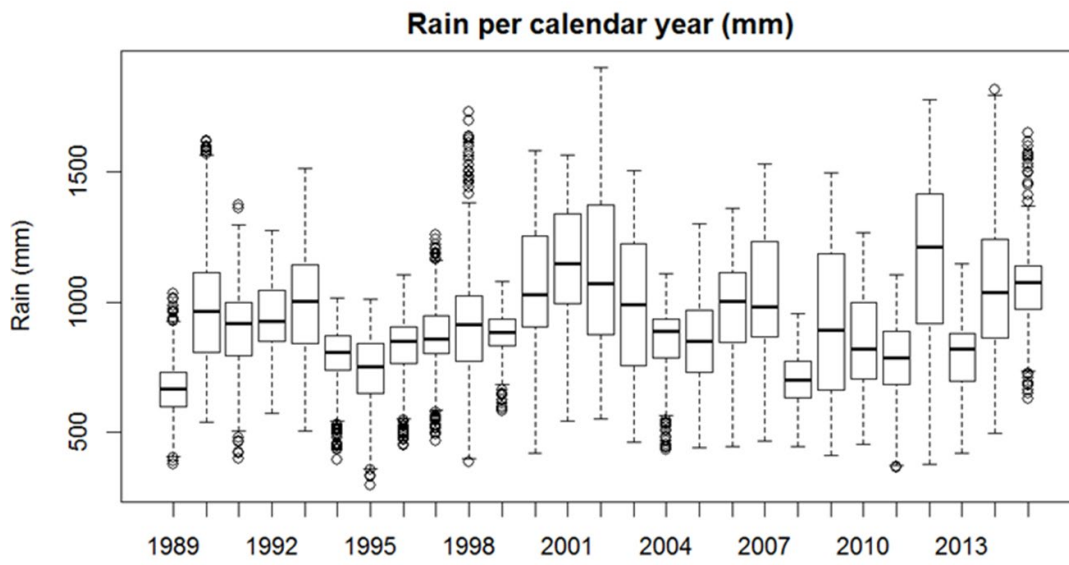


Fig. 4 Rainfall (mm yr^{-1}) in the Pampas for the years 1989 – 2015; values are given with a spatial variation as boxplots with median, quartile and extreme rainfall within all grids applied for the distributed modelling.

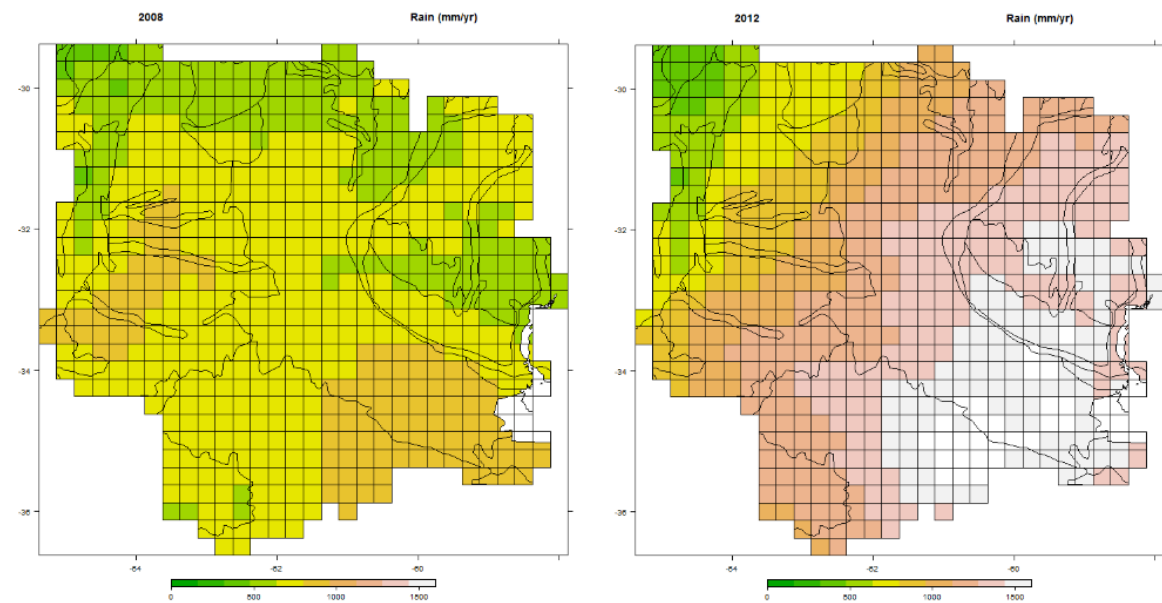


Fig. 5 Rainfall (mm yr^{-1}) in the dry year 2008 (left) and in the wet year 2012 (right)

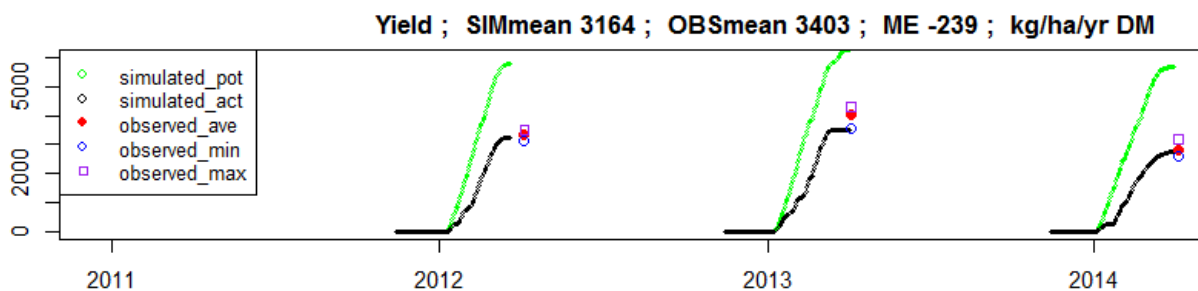


Fig. 6. Results for soybean at the Zavalla site: simulated and observed harvested yields of soy beans (kg ha^{-1} dry matter) for the calibration years 2011-2014

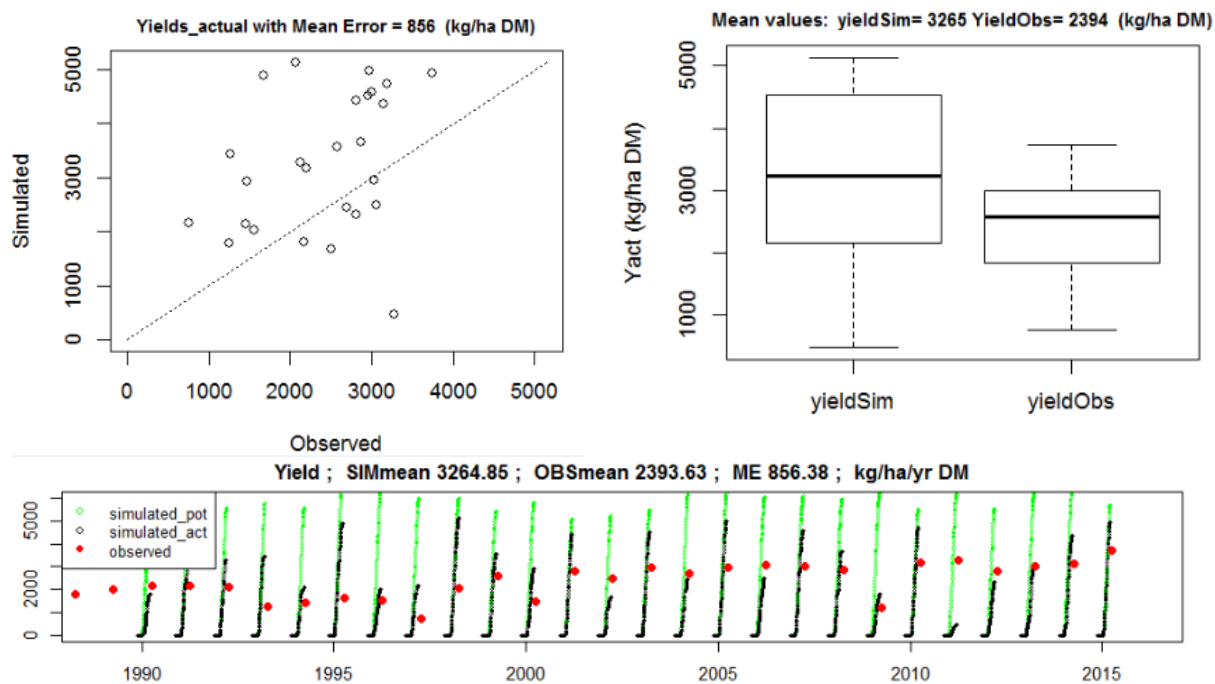


Fig. 7. Results for soybean at the site Zavalla: Top left graph shows simulated and observed yields (kg ha^{-1} DM) from official statistics at county level for the period 1990-2015. Top right shows boxplot with median, quartile and extreme values. Lower graph shows the actual yields (kg ha^{-1} DM) during the period 1990-2015

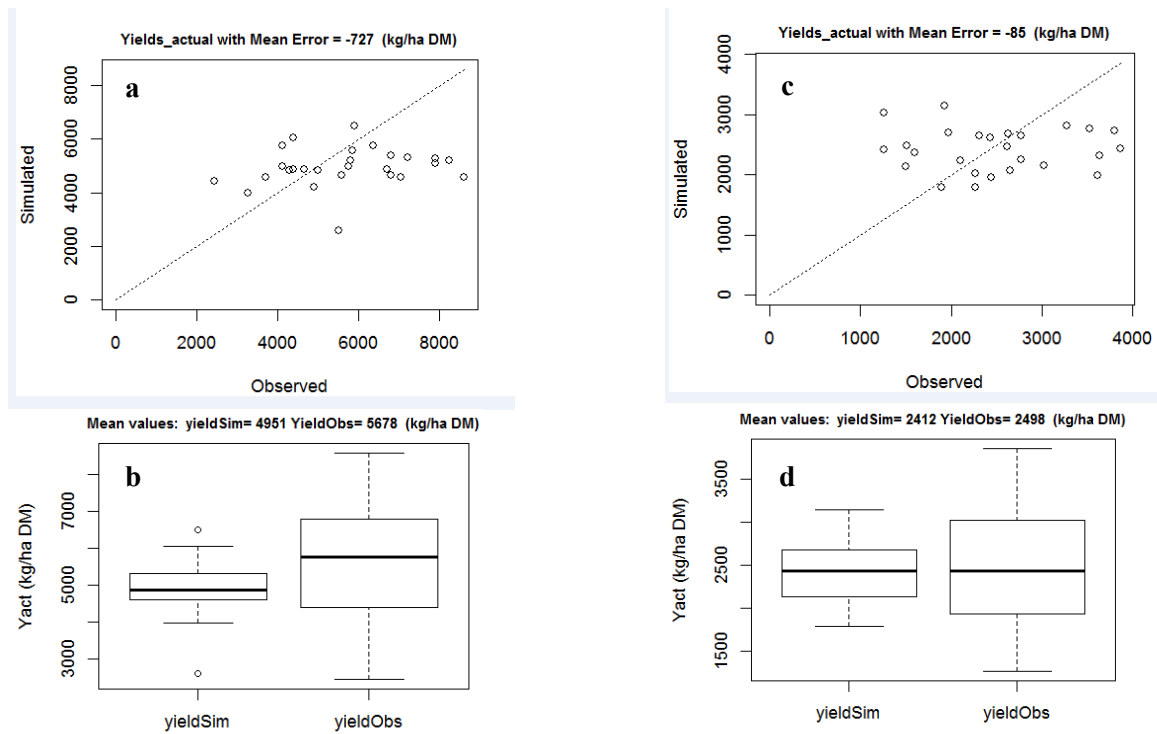


Fig. 8. Results for grain maize (a and b) and wheat (c and d) in San Antonio: Upper graphs show simulated and observed yields (kg ha⁻¹ DM) from official statistics at county level for the period 1990-2015. Lower graph shows boxplot with median, quartile and extreme values.

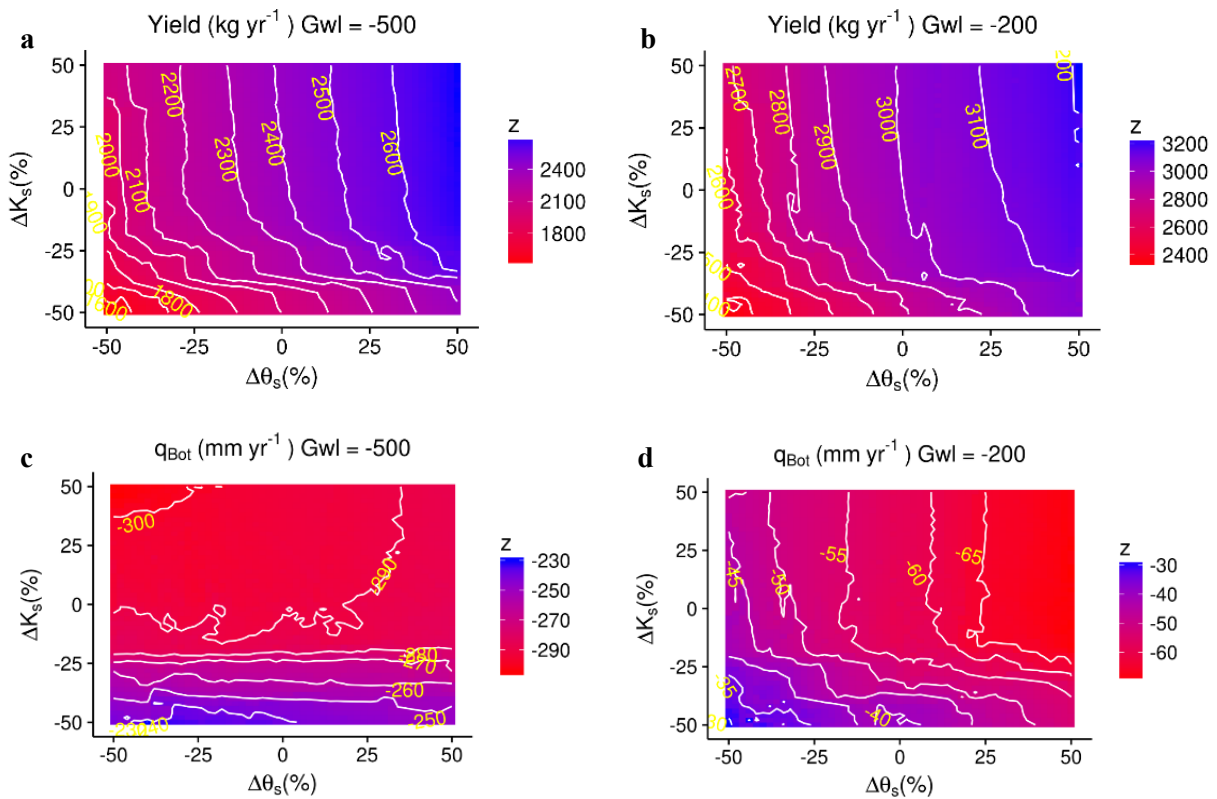


Fig. 9. Results of the sensitivity analysis: Impact on yield (kg ha⁻¹ yr⁻¹) of K_s and Θ_s using a groundwater level at an average depth of 500 cm (a) and 200 cm (b), and impact on groundwater recharge or bottom boundary flux (q_{bot} in mm yr⁻¹) using a groundwater level at an average depth of 500 cm (c) and 200 cm (d).

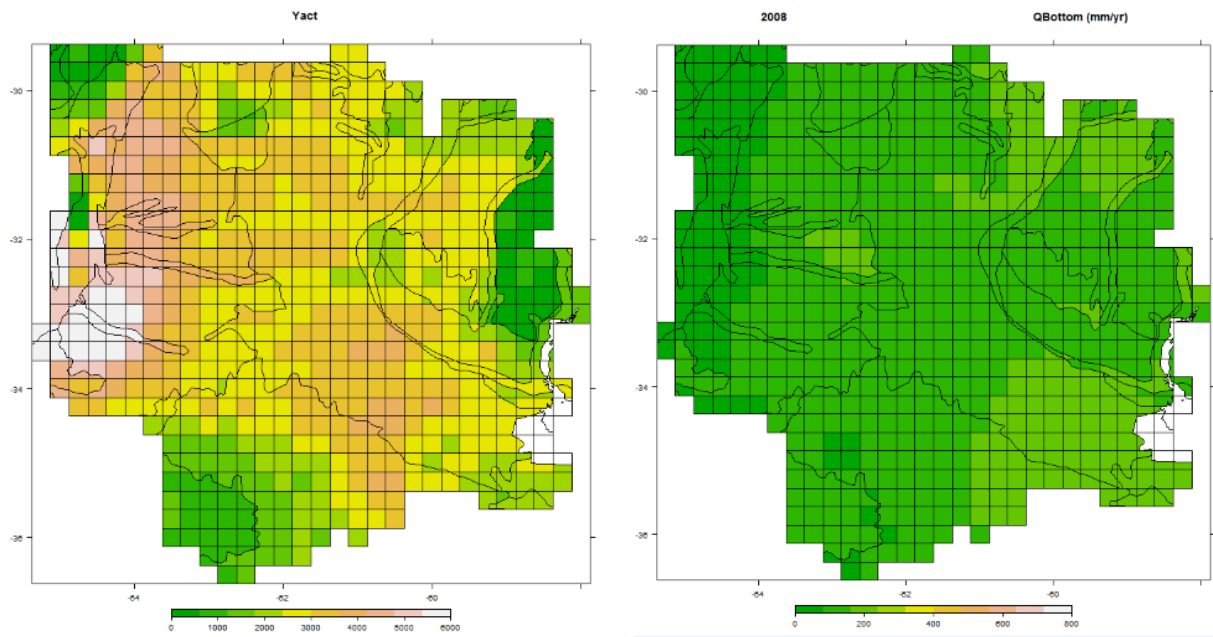


Fig. 10. Dry year 2008: Actual Yields ($\text{kg ha}^{-1} \text{ DM}$) (left) and groundwater recharge (mm yr^{-1})

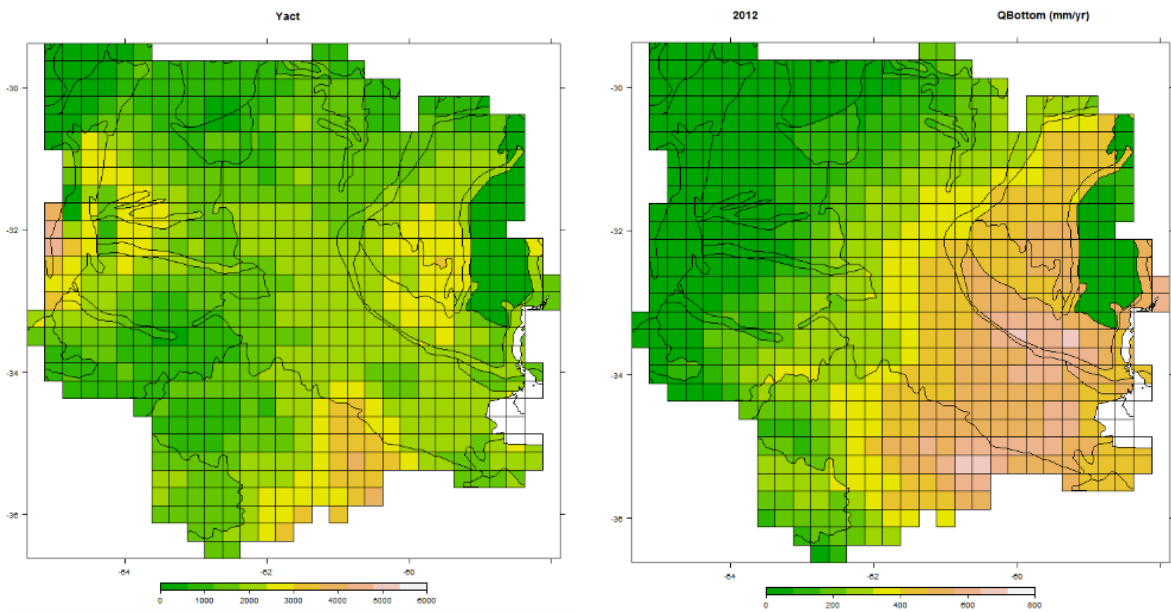


Fig. 11. Wet year 2012: Actual Yields ($\text{kg ha}^{-1} \text{ DM}$) (left) and groundwater recharge (mm yr^{-1})

q_{vert} bottom rootzone (mm crop season⁻¹)

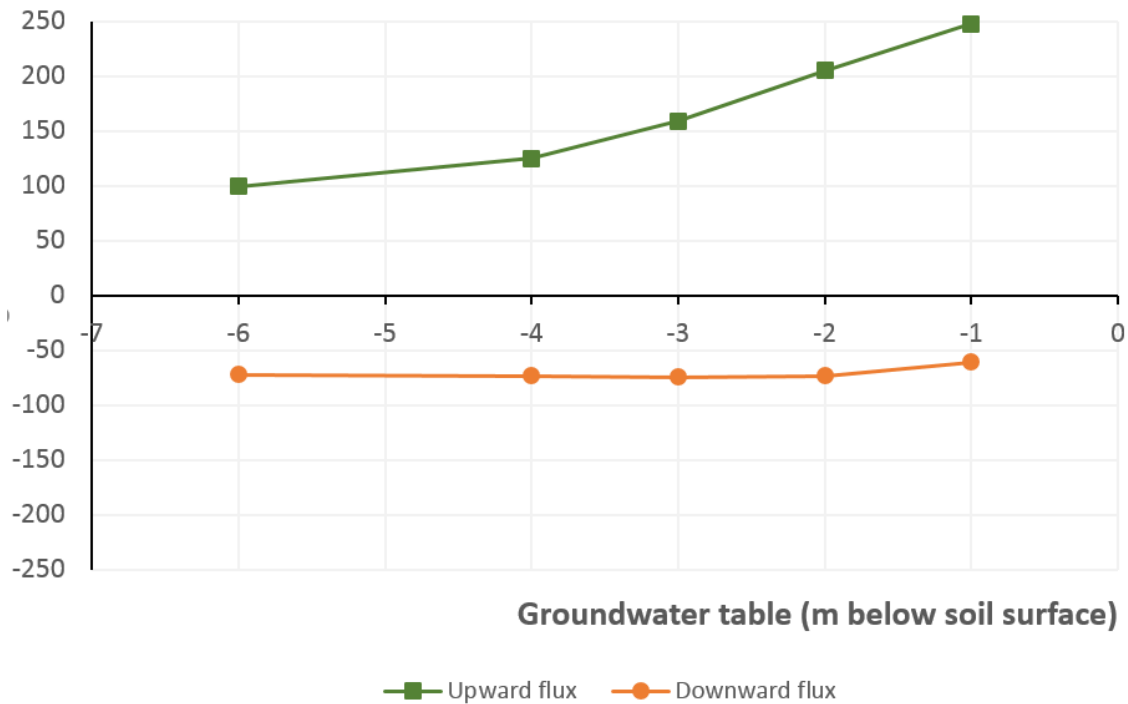


Fig. 12. Vertical water flux (q_{vert} in mm crop season⁻¹) across the lower boundary of the root zone as function of average groundwater table (m below soil surface); results for 5 different hydrological lower boundary condition; upward flux is positive, downward flux is negative.

Yield actual (kg ha⁻¹ DM)

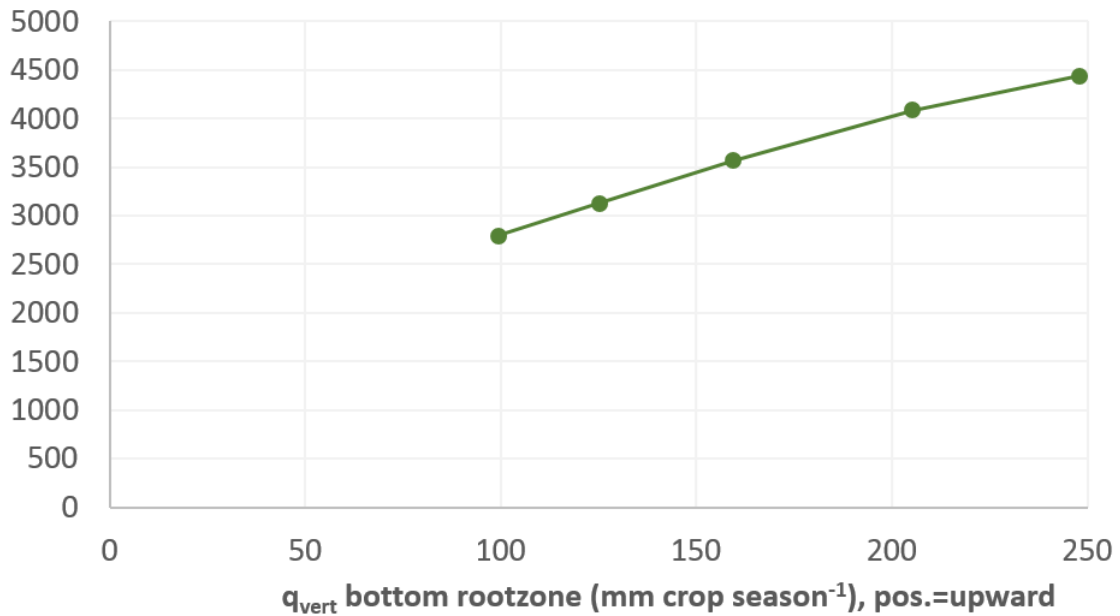


Fig. 13. Average actual yields (in kg ha⁻¹ DM) as function of upward water flux (mm crop season⁻¹) across the lower boundary of the root zone

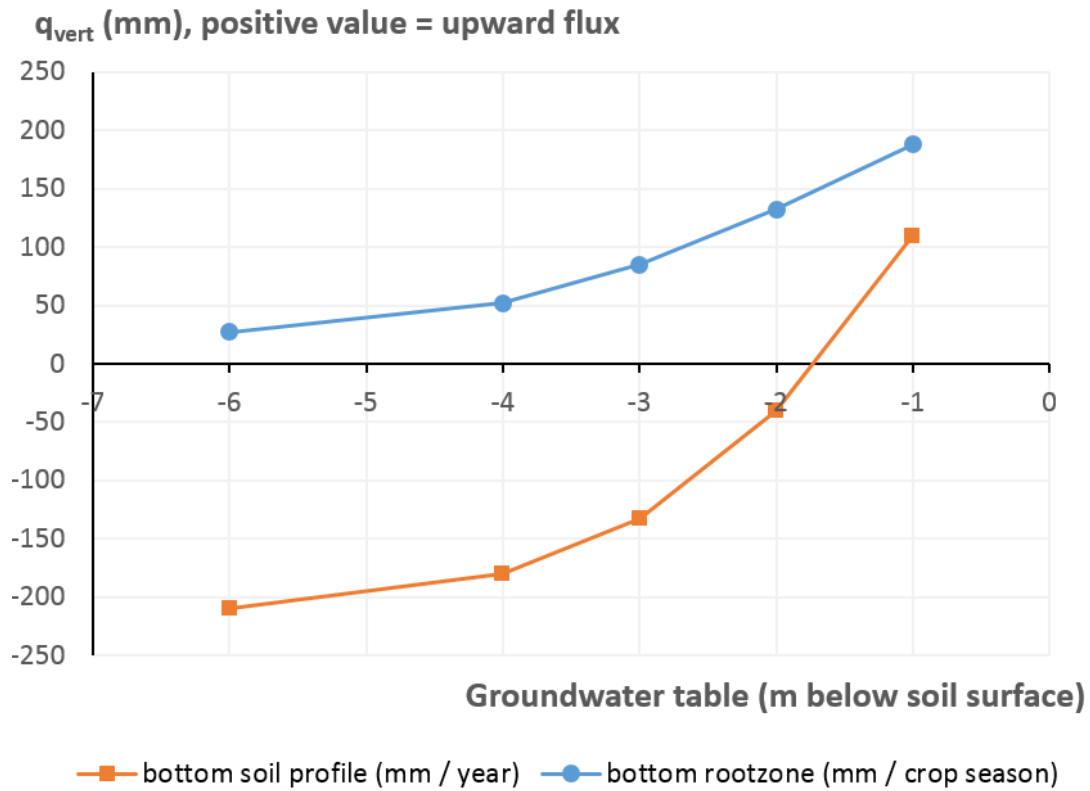


Fig. 14. Vertical water flux q_{vert} (mm) across the lower boundary of the root zone (upper figure) and across the lower boundary of the soil profile (lower figure) as function of average groundwater table (m below soil surface); results for 5 different hydrological lower boundary condition; upward flux is positive, downward flux is negative.

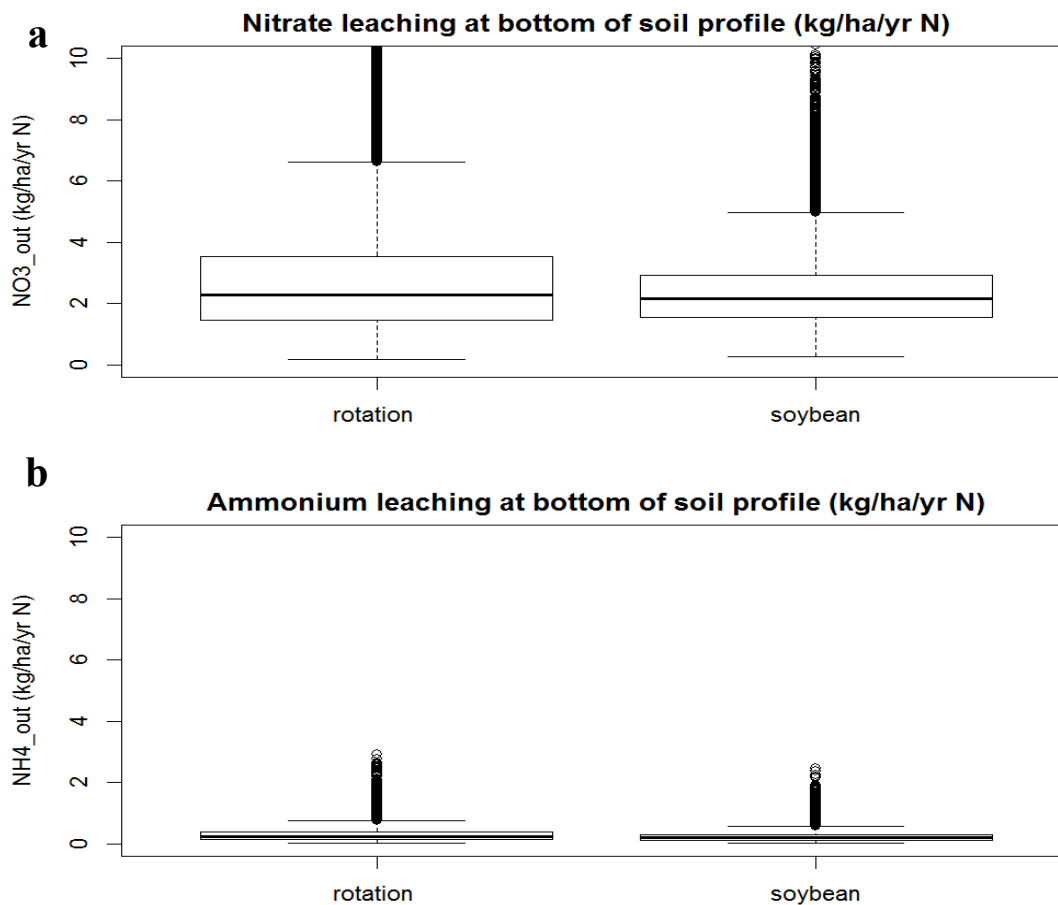
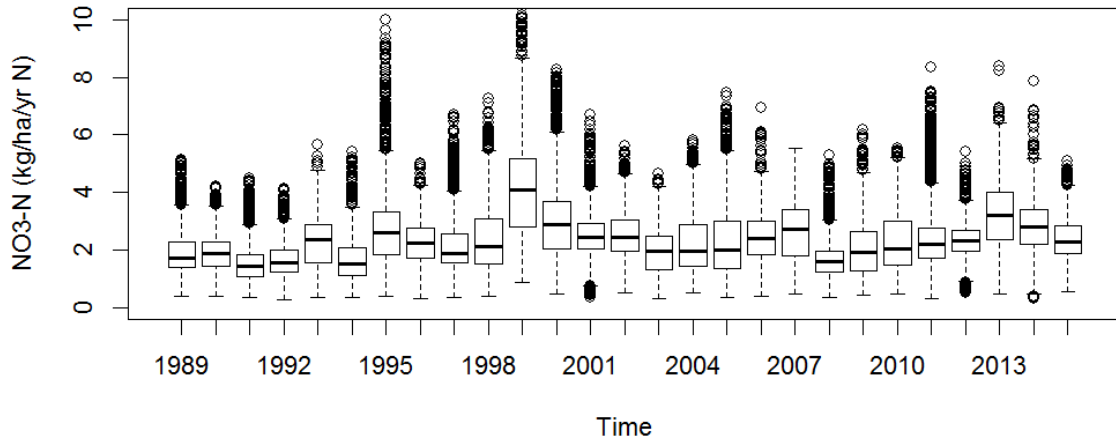


Fig. 15. Boxplots with results of downward leaching flux ($\text{kg ha}^{-1} \text{ yr}^{-1} \text{ N}$) of $\text{NO}_3\text{-N}$ (a) and $\text{NH}_4\text{-N}$ (b) across bottom of soil profile below crop rotation (left) and soybean (right) under free-drainage conditions.

a



b

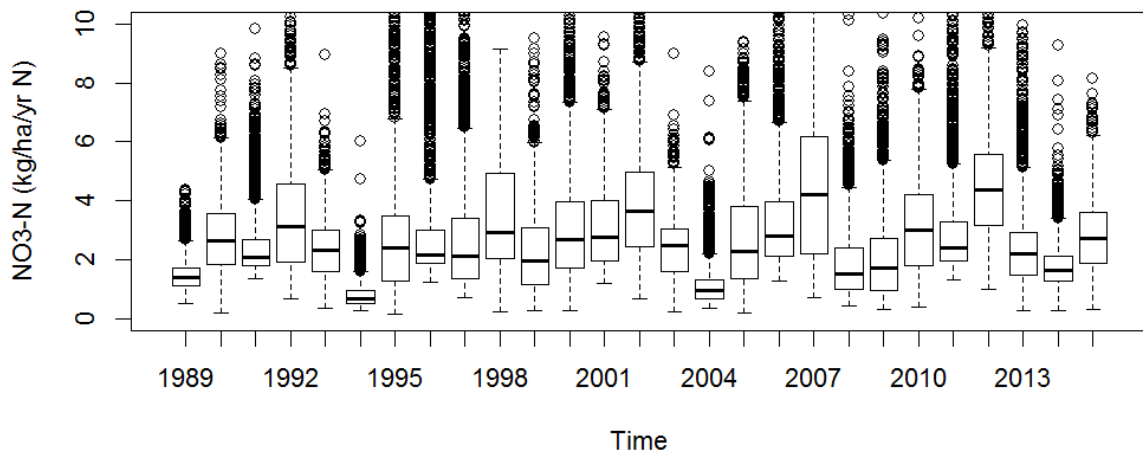


Fig. 16. Boxplots with results of downward downward leaching $\text{NO}_3\text{-N}$ flux ($\text{kg ha}^{-1} \text{ yr}^{-1} \text{ N}$) across bottom of soil profile below soybean (a) and crop rotation (b).

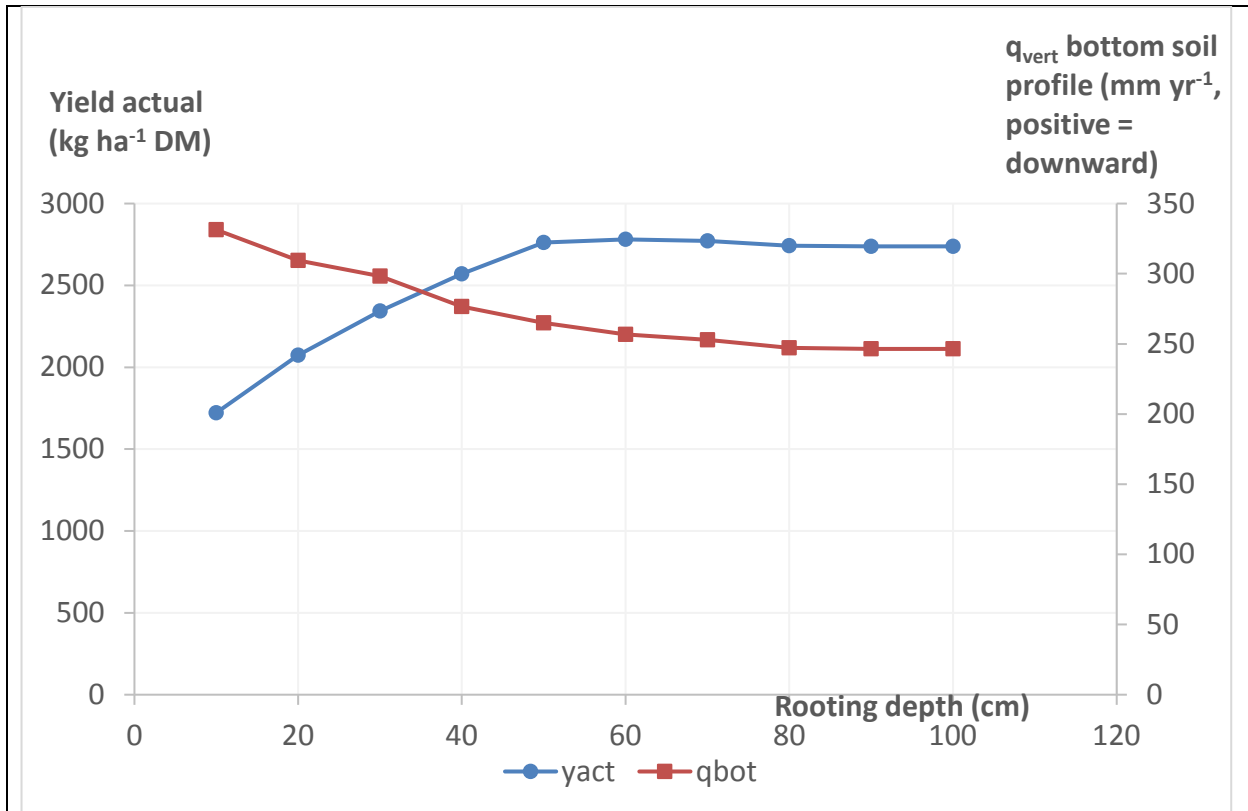


Fig. 17. Results of limited rooting depth on actual yield and on groundwater recharge q_{Bot} . Actual yield (kg ha⁻¹ DM) and groundwater recharge as flux across bottom of soil profile ($q_{Bot} = q_{vert}$ in mm yr⁻¹) as function of maximum rooting depth (cm)